AFRL-SR-AR-TR-04-

0308

REPORT DOCUMENTATION PAGE

1. REPORT DATE *(DD-MM-YYYY)*	2. REPORT TYPE	3. DATES COVERED *(From - To)*
	Final	1 Sep 2002 - 31 Dec 2003

4. TITLE AND SUBTITLE
Cluster Orbits With Perturbations of Keplerian Elements Equations

5a. CONTRACT NUMBER

5b. GRANT NUMBER
F49620-02-1-0411

5c. PROGRAM ELEMENT NUMBER

6. AUTHOR(S)
Craig A. McLaughlin

5d. PROJECT NUMBER

5e. TASK NUMBER

5f. WORK UNIT NUMBER

7. PERFORMING ORGANIZATION NAME(S) AND ADDRESS(ES)
The University of North Dakota
4149 Campus Road
Grand Forks, ND 58202-9008

8. PERFORMING ORGANIZATION REPORT NUMBER

9. SPONSORING/MONITORING AGENCY NAME(S) AND ADDRESS(ES)
Air Force Office of Scientific Research
4015 Wilson Blvd
Mail Room 713
Arlington, VA 22203

10. SPONSOR/MONITOR'S ACRONYM(S)
AFOSR

11. SPONSOR/MONITOR'S REPORT NUMBER(S)

12. DISTRIBUTION/AVAILABILITY STATEMENT
Distribution Statement A. Approved for public release; distribution is unlimited

20040625 134

13. SUPPLEMENTARY NOTES

14. ABSTRACT
This effort was performed jointly with Chris Sabol of AFRL/DEBI. The Cluster Orbit with Perturbations of Keplerian Elements (COWPOKE) Equations were developed. The initial COWPOKE equations described the relative motion of space objects in non-circular orbits using Keplerian elements. Modifications to the equations were made and the equations were used in a relative orbit determination scheme to show the benefits of relative orbit determination for satellites collocated in a single geosynchronous orbit slot. Finally, initial work was done to add Earth oblateness and drag perturbations to the COWPOKE equations.

15. SUBJECT TERMS

16. SECURITY CLASSIFICATION OF:			17. LIMITATION OF ABSTRACT	18. NUMBER OF PAGES	19a. NAME OF RESPONSIBLE PERSON
a. REPORT	b. ABSTRACT	c. THIS PAGE			Craig A. McLaughlin
U	U	U	UU		19b. TELEPHONE NUMBER *(Include area code)* 701-777-3711

Title: Cluster Orbits With Perturbations of Keplerian Elements Equations
Grant: F49620-02-1-0411, 1 September 2002-31 December 2003

PI: Craig A. McLaughlin
Phone: (701) 777-6790, FAX: (701) 777-3711
Mailing Address: University of North Dakota, Space Studies Department, 4149 Campus Road, Grand Forks, ND 58202-9008
E-Mail Address: craigm@space.edu
AFOSR Program Manager: Dr. Fariba Fahroo

Research Objective:
Express the perturbed equations of relative motion for space objects in non-circular orbits using Keplerian elements and low order expansions

Summary

This effort was performed jointly with Chris Sabol of AFRL/DEBI. The Cluster Orbit with Perturbations of Keplerian Elements (COWPOKE) Equations were developed. The initial COWPOKE equations described the relative motion of space objects in non-circular orbits using Keplerian elements. Modifications to the equations were made and the equations were used in a relative orbit determination scheme to show the benefits of relative orbit determination for satellites collocated in a single geosynchronous orbit slot. Finally, initial work was done to add Earth oblateness and drag perturbations to the COWPOKE equations

Publications:

Catlin, K., "Satellite Formation Flight Using the Perturbed COWPOKE Equations," *AIAA Region V Student Conference*, Minneapolis, MN, 28-30 April, 2004

Hill, K., C. Sabol, C. A. McLaughlin, K. K. Luu, M. M. Murai, "Relative Orbit Determination of Geosynchronous Satellites Using the COWPOKE Equations," *AAS/AIAA Space Flight Mechanics Meeting*, Maui, HI, 8-12 February 2004.

Hill, K., C. Sabol, K. K. Luu, M. M. Murai, C. A. McLaughlin, "Relative Orbit Trajectories of Geosynchronous Satellites Using the COWPOKE Equations," *Proceedings of the AMOS Technical Conference*, Maui, HI, 11 September 2003.

Sabol, C., C. A. McLaughlin, K. K. Luu, "Meet the Cluster Orbits with Perturbations of Keplerian Elements (COWPOKE) Equations," AAS 03-138, *Space Flight Mechanics 2003*, Vol. 114 of *Advances in the Astronautical Sciences*, Ponce, Puerto Rico, 9-13 February 2003, pp. 573-594.

Meet the Cluster Orbits With Perturbations Of Keplerian Elements (COWPOKE) Equations

Chris Sabol[1], Craig A. McLaughlin[2], and K. Kim Luu*

Recent developments have indicated that it is possible to express the relative equations of motion for space objects in non-circular orbits using mean Keplerian elements and low order expansions. This paper provides the initial derivation of one such effort known as the Cluster Orbits With Perturbations Of Keplerian Elements (COWPOKE) equations. Given mean Keplerian elements and element differences, the COWPOKE equations describe spherical radial, cross-track, and along-track separations of the satellites as an explicit function of time. The framework of the equations allows for very high eccentricity reference orbits and for the inclusion of dynamic perturbations. Test cases using two-body dynamics show the utility of this approach.

INTRODUCTION

Cluster orbits are defined as the relative trajectories of objects traveling through space in close proximity to each other. Clusters occur when satellites in similar orbits approach each other, groups of satellites fly in formation to perform specific mission functions, or several objects are launched or deployed from the same object. Each case has its own unique nuances, but the dynamics of how the objects move relative to each other are functionally the same.

The number of satellites in the geosynchronous belt has been steadily increasing for almost 40 years. While the number of satellites has been increasing, the space in the geosynchronous belt has not. This has led to more clusters of satellites operating in close proximity of each other and often unintentionally passing within kilometers of their neighbors[1]. Clusters of objects at this great altitude have been a long-standing challenge to space surveillance where the satellites can be mistaken for each other.

In recent years, there has been increasing interest in the use of satellites flying in formation. Several missions and mission statements have identified formation flying as a means of reducing cost and adding flexibility to space based programs or to accomplish goals that are not possible or very difficult to accomplish with a single satellite. These missions include NASA's Earth Observing-1 flying in formation with Landsat-7 and several European missions. In addition NASA has developed over 20 concepts for future missions involving formation flying. Many of these missions involve highly eccentric orbits.

During ballistic missile launches, several objects can achieve low earth orbit including the reentry vehicle, booster, fairings, and the possibility of several balloon-like decoys attempting to confuse missile defense systems. It is the responsibility of the missile defense system to track the cluster of objects and quickly identify the reentry vehicle.

The Cluster Orbits with Perturbations of Keplerian Elements (COWPOKE) equations can provide the theoretical foundation for analysis tools supporting a variety of applications. Optical space surveillance often reveals multiple satellites in a single telescope field of view. An understanding of the relative dynamics may allow for satellite identification based solely on relative position. Further research may apply these results to relative orbit determination of objects in a cluster or during close approach encounters. This approach may prove to be more accurate than performing orbit determination on the individual objects and determining differences. The equations might also be used to support the missile tracking experiments. If tracking sensors have limited fields of view, they may be required to track ballistic clusters individually; meaningful relative equations of motion may simplify the transition from object to object. Even if objects are tracked simultaneously, the relative equations of motion can be

[1] Air Force Research Laboratory, Directed Energy Directorate, 535 Lipoa Parkway, Suite 200, Kihei, HI 96753
[2]Space Studies Department, University of North Dakota, 4149 Campus Rd., 530 Clifford Hall, Grand Forks, ND 58202-9008

used as part of the discrimination process to identify balloon-like decoys. The COWPOKE equations would also be extremely relevant to satellite formation flying work, such as the initial Air Force Research Laboratory's TechSat 21 program, for formation flying design, analysis, and guidance and control applications. While a great deal of work has already been completed in support of formation flying missions, none provide the level of intuition and understanding as one that uses Keplerian elements. In addition, none of the work is accurate for long-term relative motion for orbits with eccentricities up to 0.7.

A simple set of equations describing the relative motion of spacecraft clusters is needed for analysis, design, and/or tracking of clusters. Much of the previous work in this field has relied on using Hill's equations[2] (also known as the Clohessy-Wiltshire equations[3]). Hill's equations describe the relative motion of spacecraft using a spacecraft-centered coordinate system. However, Hill's equations assume that the reference orbit is circular, the objects are close together, and there are no perturbations to simple two-body motion. Several researchers have pointed out the severe limitations inherit in these assumptions. To rectify this, Gim and Alfriend[4] used energy methods to develop a state transition matrix to describe relative motion in non-circular orbits under the influence of perturbations. While closed form analytic solutions in a transformed variable space are valuable for analysis, these approaches may be awkward for many applications since transformations are required to go from the canonical variable space to more traditional representations of satellite orbits such as Keplerian elements. Additionally, most working level engineers lack the background to implement this approach. Previous work by Garrison et al.[5] developed equations of motion for elliptical orbits in terms of the true anomaly instead of time. Also, these equations were developed with rendezvous in mind and are developed only to second order in eccentricity. In addition, Melton[6] developed a state transition matrix for relative motion in eccentric orbits that is time dependent. Melton relied on some of the same foundations that are used in this paper, but the development was only to second order in eccentricity and is not accurate for orbits of high eccentricity. Baoyin et al,[12] did similar work but assumed matching orbital periods; this work also provides physical insight into formation flying in near circular orbits. This paper develops physically meaningful equations of relative motion for space objects in non-circular orbits using Keplerian elements.

Previous work by the authors[7] led to the development of a set of equations that describe the first order effects of Earth oblateness on the relative motion of objects in circular orbits. In addition, they developed a simple set of equations to describe the effects of Earth oblateness for polar orbits. Then, they further developed the equations to describe the motion for all inclinations[8]. Finally, they examined the long-term evolution of the relative motion for circular orbits and presented an approach to describe relative motion of satellites in elliptical orbits without perturbations and assuming matching periods[9]. This last step provided the building blocks for the COWPOKE equations.

In the past, equations of relative motion such as Hill's equations were developed by differencing the quasi-inertial equations of motion and mapping those differences into the rotating coordinate system. The result was a set of equations that describe the relative differences between the satellites typically in terms of radial, cross-track, and along-track components. Rather than using the traditional algebraic approach, the COWPOKE equations are developed using a geometric approach. Here, the geometric properties and definitions of Keplerian orbital elements will be used directly to map orbital element differences into the radial, cross-track, and along-track relative motion. In addition to the increased intuitiveness of a geometric approach, by using Keplerian orbital elements and differences in those orbital elements, we can take advantage of existing perturbation model development and incorporate meaningful dynamics into the relative equations of motion much easier than with the algebraic approaches.

There are challenges to this approach. First and foremost, the geometric properties of Keplerian elements are a function of the true anomaly, which has non-uniform variation with time. Ideally, analytical solutions are expressed in terms of the mean anomaly, which does vary linearly with time (outside the influence of perturbations). The relationship between the mean anomaly and eccentric anomaly is given by the well- known transcendental Kepler's equation. This research uses a series expansion to approximate the true anomaly as a function of time. A relation of this sort was successfully employed as part of the building blocks of the COWPOKE equations.

Using that one relationship, one can construct the relative motion of formation flying satellites by reconstructing the orbits individually based on their Keplerian elements and then differencing the two. This paper develops true equations of relative motion for clusters of objects. And, unlike the previous work, this research incorporates

perturbation models and be generalized to account for small differences in semimajor axis. This results in a set of equations that describe the radial, cross-track, and along-track differences between two space objects in formation or a cluster based on Keplerian orbital element differences.

APPROACH

The formulation of the COWPOKE equations has three major challenges. The first is choosing a suitable reference frame for the relative equations of motion and expressing that frame in terms of Keplerian elements and element differences. The second is representing the geometrical true anomaly as a function of time. The final challenge is incorporating relevant perturbation effects. Only the first two challenges are addressed in this work.

Classical relative motion approaches use a Cartesian reference frame to describe relative motion. The components of this frame are radial, cross-track, and along-track differences. A limitation of this approach is that significant cross-mapping between components occurs when the separation distance between the satellites is not small. For instance, if two satellites travel together in a circular orbit but are separated by 0.01 rad in true anomaly, the relative position of one satellite with respect to the other will have an along-track separation as anticipated but will also have a radial component despite the fact that the satellites are at the same altitude and within the same orbit. Relative position difference components that are artifacts of the chosen coordinate frame, such as the one outlined in the preceding example, can greatly complicate the analysis of the relative motion.

A second coordinate frame choice is to use spherical separations. Here, the relative position difference is described by an altitude difference from a sphere having the radius of the reference satellite and angular components perpendicular to and along the reference satellite's direction of motion projected onto the sphere. These components, δr, δxt, and δat, are illustrated in Figure 1. The spherical reference frame is well-suited to describing the position of satellites in circular or near-circular orbits; however, when the orbital eccentricity becomes large, the spherical reference frame suffers from the same limitations as the Cartesian system.

A third option to describe the relative motion of satellites in elliptic orbits is to use an ellipsoidal reference system. This is similar to the spherical system except that the components are mapped along an ellipsoid rather than a sphere. This method has geometric challenges describing altitude variations and can still result in difficult to understand position differences.

For this formulation, we chose the spherical reference frame since it's slightly better than Cartesian for describing the orbital motion and provides the physical insight we desire. Additionally, it is a simple geometric mapping between spherical and Cartesian given the quantities described in this work if Cartesian coordinates are desired. In fact, the desired reference frame will likely be a function of application, but it is hoped that enough information is provided here so these equations can be easily reformulated in other reference frames.

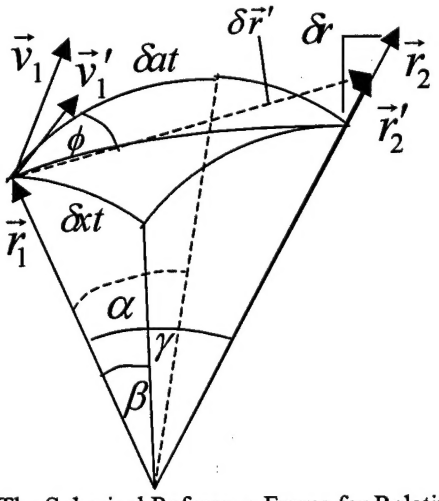

Figure 1: The Spherical Reference Frame for Relative Motion

The spherical coordinate system used here can be realized using position and velocity vectors of the two satellites:

$$\cos(\gamma) = \frac{\vec{r}_1 \bullet \vec{r}_2}{r_1 r_2}$$

$$r_2' = \frac{r_1}{\cos(\gamma)}$$

$$\vec{r}_2' = \left(\frac{\vec{r}_2}{r_2}\right) r_2'$$

$$\delta\vec{r}' = \vec{r}_2' - \vec{r}_1$$

$$\vec{v}_1' = \vec{v}_1 - \left(\frac{\vec{v}_1 \bullet \vec{r}_1}{r_1}\right)\frac{\vec{r}_1}{r_1}$$

$$\cos(\phi) = \frac{\delta\vec{r}' \bullet \vec{v}_1'}{\delta r' v_1'}$$

$$\sin(\beta) = \sin(\gamma)\sin(\phi)$$

$$\cos(\alpha) = \frac{\cos(\gamma)}{\cos(\beta)}$$

$$\begin{aligned} \delta r &= r_2 - r_1 \\ \delta xt &= r_1\beta \\ \delta at &= r_1\alpha \end{aligned} \qquad (1)$$

Here, the auxiliary vector quantities, denoted by primes, are introduced so right planar triangles can be used in the determination of desired angular values. The spherical components can be expressed in terms of Keplerian elements by using the following definitions[10]:

$$\vec{r} = \frac{a(1-e^2)}{1+e\cos(f)}\begin{bmatrix} \cos(\Omega)\cos(\omega+f) - \sin(\Omega)\sin(\omega+f)\cos(i) \\ \sin(\Omega)\cos(\omega+f) - \cos(\Omega)\sin(\omega+f)\cos(i) \\ \sin(\omega+f)\sin(i) \end{bmatrix} \qquad (2)$$

$$\vec{v} = \frac{-\mu}{\sqrt{\mu a(1-e^2)}}\begin{bmatrix} \cos(\Omega)(\sin(\omega+f)+e\sin(\omega)) + \sin(\Omega)(\cos(\omega+f)+e\cos(\omega))\cos(i) \\ \sin(\Omega)(\sin(\omega+f)+e\sin(\omega)) + \cos(\Omega)(\cos(\omega+f)+e\cos(\omega))\cos(i) \\ -(\cos(\omega+f)+e\cos(\omega))\sin(i) \end{bmatrix}$$

However, the resulting equations become difficult to manipulate. Instead, a simple geometrical mapping of Keplerian element and element differences into the spherical components of relative motion can be achieved with the following:

$$\delta r = \frac{(a_1+\delta a)(1-(e_1+\delta e)^2)}{1+(e_1+\delta e)\cos(f_1+\delta f)} - \frac{a_1(1-e_1^2)}{1+e_1\cos(f_1)}$$

$$\delta xt/r_1 = \beta = -\delta\Omega\sin(i_1)\cos(\omega_1+\delta\omega+f_1+\delta f) + \delta i\sin(\omega_1+\delta\omega+f_1+\delta f) \qquad (3)$$

$$\delta at / r_1 = \alpha = (\delta\omega + \delta f)\cos(\delta i) + \delta\Omega\cos(i_1)$$

The spherical cross-track and along-track terms are, in fact, approximations accurate to first order in the Keplerian elements differences. Figure 2 illustrates how these terms are derived.

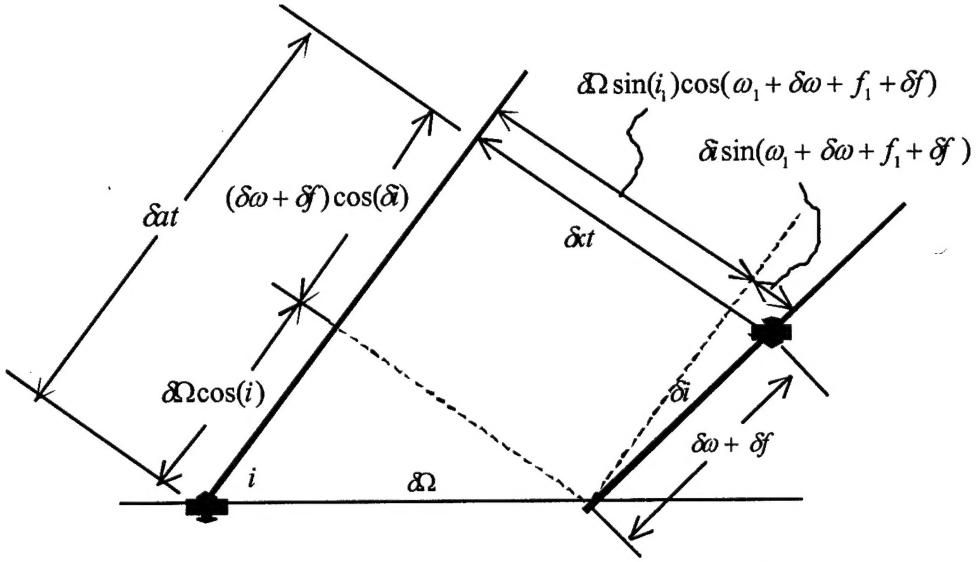

Figure 2: Spherical Components in Terms of Keplerian Elements and Element Differences

We can further simplify the radial expression to first order in the Keplerian element differences:

$$\delta r = \frac{1-e_1^{\,2}}{1+e_1\cos(f_1)}\delta a + \frac{-a(2e_1+(1+e_1^{\,2})\cos(f_1))}{(1+e_1\cos(f_1))^2}\delta e + \frac{a_1 e_1(1-e_1^{\,2})\sin(f_1)}{(1+e_1\cos(f_1))^2}\delta f \qquad (4)$$

From these Keplerian element representations of the relative motion, we can derive some physical insight into how orbital differences result in relative motion. If we assume a circular reference orbit, Eqs. (3) and (4) resemble the solutions to Hill's equations where the cross-track motion becomes a simple oscillation, the altitude difference maps directly into the radial motion with a periodic variation introduced by the eccentricity, and the altitude difference couples into the along-track component through the true anomaly resulting in a combination of secular and periodic effects[7].

While the equations above are useful and do help provide physical insight into the relative motion, they are expressed in terms of true anomaly. To express the relative motion as a function of time, one must express the above equations in terms of mean anomaly. At a fundamental level, this entails finding a suitable approximate solution to Kepler's equation. Battin provides several methods for doing so[10]. For the initial COWPOKE development, it was decided to use a Fourier-Bessel expansion of the true anomaly in terms of the mean anomaly and eccentricity.

Using the geometric properties of the true and eccentric anomalies and Kepler's equation, the following relationship can be found:

$$\frac{df}{dM} = \frac{\sqrt{1-e^2}}{(1-e\cos E)^2} \qquad (5)$$

This can be expressed in terms of a Fourier cosine series that introduces the Bessel functions, J_n:

$$\frac{df}{dM} = \sqrt{1-e^2}\left(B_0 + \sum_{k=1}^{\infty} B_k \cos(kM)\right),\ B_0 = \frac{1}{\sqrt{1-e^2}}, \tag{6}$$

$$B_k = \frac{2}{\sqrt{1-e^2}} \sum_{n=-\infty}^{\infty} \mathrm{J}_n(-ke)\beta^{|k+n|},$$

$$\mathrm{J}_n(-ke) = (-ke)^n \sum_{m=0}^{\infty} \frac{(-1)^m (-ke)^{2m}}{2^{2m+n}\, m!(n+m)!},$$

$$\beta = \frac{1-\sqrt{1-e^2}}{e},\ \beta^{|k+n|} = \left(\frac{e}{2}\right)^{|k+n|}\left[1 + \sum_{l=1}^{\infty}\left(\frac{e}{2}\right)^{2l} \frac{|k+n|}{l!} \prod_{j=1}^{l-1}\left(|k+n| + 2l - j\right)\right]$$

Integrating this equation with respect to the mean anomaly provides an expression for the true anomaly in terms of the mean anomaly:

$$f = M + 2\sum_{k=1}^{\infty} \frac{1}{k}\left[\sum_{n=-\infty}^{\infty} \mathrm{J}_n(-ke)\beta^{|k+n|}\right]\sin(kM) \tag{7}$$

The result of this expansion is a sine series with coefficients that are power series in eccentricity. The lowest order of eccentricity for each coefficient series is k; thus the upper limit for k can be chosen based on the eccentricity of the reference orbit and the desired accuracy. Figure 3 plots eccentricity to the (k+1) power. The figure is meant to provide an indicator for the relative accuracy of Eq. (7) for a given eccentricity and choice of k. For instance, if one had a references eccentricity of 0.3 and desired series truncation errors below 1%, then one would choose to truncate the series at k=4 or the fourth power of eccentricity. When k=8, one sees errors below 10% up to e=0.7.

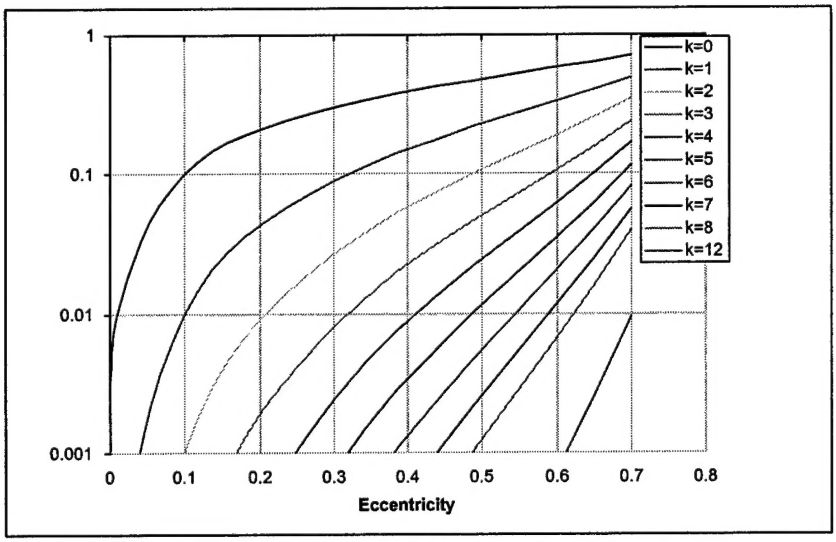

Figure 3: Relative Error Order of Magnitude for Eccentricity Series

Evaluating Eq. (7) up to the ninth frequency term (8M) yields:

$$f = M + \left(2e - \frac{1}{4}e^3 + \frac{5}{96}e^5 + \frac{107}{4608}e^7\right)\sin(M) + \left(\frac{5}{4}e^2 - \frac{11}{24}e^4 + \frac{17}{192}e^6 + \frac{43}{5760}e^8\right)\sin(2M) +$$
$$\left(\frac{13}{12}e^3 - \frac{43}{64}e^5 + \frac{95}{512}e^7\right)\sin(3M) + \left(\frac{103}{96}e^4 - \frac{451}{480}e^6 + \frac{4123}{11520}e^8\right)\sin(4M) +$$
$$\left(\frac{1097}{960}e^5 - \frac{5957}{4608}e^7\right)\sin(5M) + \left(\frac{1223}{960}e^6 - \frac{1987}{1120}e^8\right)\sin(6M) +$$
$$\left(\frac{47273}{32256}e^7 - \frac{12412897}{5160960}e^9\right)\sin(7M) + \left(\frac{556403}{322560}e^8 - \frac{4745483}{1451520}e^{10}\right)\sin(8M) \quad (8)$$

In examining Eq. (8), one can see that the leading term in each of the eccentricity series does not decrease for all eccentricities; however, the second term in the eccentricity series is always negative and serves to reduce the magnitude of that frequency's contribution to the expansion as a whole. Thus, the amplitude of each frequency term decreases as the frequency increases allowing convergence of the entire expansion if enough terms are included in each individual eccentricity series. This means that for higher values of eccentricity, it is very important to include at least two or more terms for each eccentricity series. In Eq. (8), if the e^9 and e^{10} terms were left out of the $7M$ and $8M$ frequency terms, the error due to this truncation could be larger than if the $7M$ and $8M$ terms were not included at all. For higher values of eccentricity, care must be taken to make certain that enough terms are included in each eccentricity series to ensure one is not adding error with a given frequency term. The good news is that each eccentricity series converges fairly quickly so that powers of eccentricity at lower frequencies are much less important than at higher frequencies; this means that one can get away with fewer terms in each eccentricity series even if higher frequency terms are required. Additionally, for smaller values of eccentricity, 0.3 and below, truncation becomes much less of an issue since the e^2 factor greatly reduces the impact of the higher order terms in each eccentricity series and each higher frequency.

Truncation issues aside, the Fourier-Bessel series expansion of the true anomaly is an important component to the formulation of the COWPOKE equations; however, an additional step must be taken to map mean anomaly differences into true anomaly differences. This is accomplished by simply applying a first order perturbation to Eq. (8):

$$\delta f = \frac{\partial f}{\partial M}\delta M + \frac{\partial f}{\partial e}\delta e \tag{9}$$

The general formulation includes higher order element difference terms and coupling terms between the element differences but for cluster orbits, including the first order terms should provide accuracy to two orders of magnitude smaller than the separation distance. Including only the first order difference terms for the true anomaly expression yields:

$$\begin{aligned}
\delta f = &\left[1+\left(2e_1-\frac{1}{4}e_1^{\,3}+\frac{5}{96}e_1^{\,5}+\frac{107}{4608}e_1^{\,7}\right)\cos(M_1)+\right.\\
&2\left(\frac{5}{4}e_1^{\,2}-\frac{11}{24}e_1^{\,4}+\frac{17}{192}e_1^{\,6}+\frac{43}{5760}e_1^{\,8}\right)\cos(2M_1)+3\left(\frac{13}{12}e_1^{\,3}-\frac{43}{64}e_1^{\,5}+\frac{95}{512}e_1^{\,7}\right)\cos(3M_1)+\\
&4\left(\frac{103}{96}e_1^{\,4}-\frac{451}{480}e_1^{\,6}+\frac{4123}{11520}e_1^{\,8}\right)\cos(4M_1)+5\left(\frac{1097}{960}e_1^{\,5}-\frac{5957}{4608}e_1^{\,7}\right)\cos(5M_1)+\\
&6\left(\frac{1223}{960}e_1^{\,6}-\frac{1987}{1120}e_1^{\,8}\right)\cos(6M_1)+7\left(\frac{47273}{32256}e_1^{\,7}-\frac{12412897}{5160960}e_1^{\,9}\right)\cos(7M_1)+\\
&\left.8\left(\frac{63643}{35840}e_1^{\,8}-\frac{4745483}{1451520}e_1^{\,10}\right)\cos(8M_1)\right]\delta M+\left[\left(2-\frac{3}{4}e_1^{\,2}+\frac{25}{96}e_1^{\,4}+\frac{749}{4608}e_1^{\,6}\right)\sin(M_1)+\right.\\
&\left(\frac{5}{2}e_1-\frac{11}{6}e_1^{\,3}+\frac{17}{32}e_1^{\,5}+\frac{43}{720}e_1^{\,7}\right)\sin(2M_1)+\left(\frac{13}{4}e_1^{\,2}-\frac{215}{64}e_1^{\,4}+\frac{665}{512}e_1^{\,6}\right)\sin(3M_1)+\\
&\left(\frac{103}{24}e_1^{\,3}-\frac{451}{80}e_1^{\,5}+\frac{4123}{1440}e_1^{\,7}\right)\sin(4M_1)+\left(\frac{1097}{192}e_1^{\,4}-\frac{41699}{4608}e_1^{\,6}\right)\sin(5M_1)+\\
&\left(\frac{1223}{160}e_1^{\,5}-\frac{1987}{140}e_1^{\,7}\right)\sin(6M_1)+\left(\frac{47273}{4608}e_1^{\,6}-\frac{12412897}{573440}e_1^{\,8}\right)\sin(7M_1)+\\
&\left.\left(\frac{63643}{4480}e_1^{\,7}-\frac{4745483}{145152}e_1^{\,9}\right)\sin(8M_1)\right]\delta e
\end{aligned} \tag{10}$$

The truncation issues for Eq. (10) are similar to those of Eq. (8) but are further compounded by the exponential factors produced when taking the partial derivative with respect to eccentricity. Note that the e^9 coefficient is twice as large as the e^7 coefficient in the $8M$ frequency series for the δe component.

For unperturbed satellite motion, we can express the mean anomaly as a function of time δM as a function of δM at epoch, semimajor axis difference, and time:

$$M_1 = M_0 + \left(\sqrt{\frac{\mu}{a_1^{\,3}}}\right)t\,,\quad \delta M = \delta M_0 + \left(\sqrt{\frac{\mu}{(a_1+\delta a)^3}}-\sqrt{\frac{\mu}{a_1^{\,3}}}\right)t \tag{11}$$

If one chooses, the mean motion terms in the above expression can be replaced by a second order perturbation of the mean motion with respect to δa without significant error for most applications:

$$\delta M = \delta M_0 + \sqrt{\mu}\left(-\frac{3}{2}a_1^{-5/2}\delta a + \frac{15}{8}a_1^{-7/2}\delta a^2\right)t \tag{12}$$

Eqs. (8), (10), and (11) can now be substituted into Eq. (3) to complete the COWPOKE equations for unperturbed satellite motion. Here are the COWPOKE equations with only first order eccentricity terms included in the expansion of the true anomaly and true anomaly difference:

$$\delta r = \frac{1-e_1^2}{1+e_1\cos(M_1+2e_1\sin(M_1))}\delta a + \frac{-a(2e_1+(1+e_1^2)\cos(M_1+2e_1\sin(M_1))}{(1+e_1\cos(M_1+2e_1\sin(M_1)))^2}\delta e +$$
$$\frac{a_1e_1(1-e_1^2)\sin(M_1+2e_1\sin(M_1))}{(1+e_1\cos(M_1+2e_1\sin(M_1)))^2}\left[(1+2e_1\cos(M_1))\left(\delta M_0+\left(\sqrt{\frac{\mu}{(a_1+\delta a)^3}}-\sqrt{\frac{\mu}{a_1^3}}\right)t\right)\right]$$

$$\delta xt/r_1 = \beta = -\delta\Omega\sin(i_1)\cos(\omega_1+\delta\omega+M_1+2e_1\sin(M_1)_1 +$$
$$\left[(1+2e_1\cos(M_1))\left(\delta M_0+\left(\sqrt{\frac{\mu}{(a_1+\delta a)^3}}-\sqrt{\frac{\mu}{a_1^3}}\right)t\right)\right]\Bigg) +$$
$$\delta i\sin(\omega_1+\delta\omega+M_1+2e_1\sin(M_1)+ \tag{13}$$
$$\left[(1+2e_1\cos(M_1))\left(\delta M_0+\left(\sqrt{\frac{\mu}{(a_1+\delta a)^3}}-\sqrt{\frac{\mu}{a_1^3}}\right)t\right)\right]\Bigg)$$

$$\delta at/r_1 = \alpha = \left(\delta\omega+\left[(1+2e_1\cos(M_1))\left(\delta M_0+\left(\sqrt{\frac{\mu}{(a_1+\delta a)^3}}-\sqrt{\frac{\mu}{a_1^3}}\right)t\right)\right]\right)\cos(\delta i)+\delta\Omega\cos(i_1)$$

Note that we have taken the linearized form of the radial component as presented in Eq. (4). From Figure 3, we would expect that these equations are accurate to the 1% level up to eccentricities of 0.1.

While this work does not currently include perturbations to the satellite dynamics, one of the key focuses of the COWPOKE development was to allow for the inclusion of additional force model effects. This can be accomplished by expressing the Keplerian elements and element differences as functions of time. This will be the focus of future work.

RESULTS

Simulations were performed to quantify the error inherent in the approximations used in the COWPOKE formulation for two test cases. The first test case employed a near-circular, low-Earth orbit (e=0.01) and the second a high altitude eccentric orbit (e=0.7). The test cases were performed in the MATLAB environment using two-body dynamics; it is understood that that these simulations only measure the effectiveness of the COWPOKE equations to model two-body motion and are not indicative of the performance for real satellite motion.

Truth data for the simulations were determined by calculating the mean anomaly of each satellite as a function of time, converting the Keplerian elements to position and velocity vectors (with an algorithm taken from Vallado[11]),

and then mapping the position differences into the spherical radial, cross-track, and along-track components described in Eq. (1). The COWPOKE results come from a direct mapping of the Keplerian element and element differences into those components using the methods described in the previous section. It should be noted that the angular cross-track and along-track values, α and β, were used for comparison purposes in the simulations rather than the arc-lengths, δxt and δat. Some additional error in the arc-lengths will be present due to the error in estimating the magnitude of the position vector of the reference satellite, but that is typically the same order of magnitude or smaller than the error in the angular separation.

Table 1 contains the orbital elements and element differences for the near-circular, low-Earth orbit (LEO) case; the reference satellite, satellite 1, has the initial Keplerian elements given in the "Reference Elements" column while the second satellite, satellite 2, has the initial Keplerian elements of the "Reference Elements" plus the "Element Differences." The simulation span covers 2 hours or just over one orbital period. The COWPOKE formulation includes only first order eccentricity terms and uses the radial component approximation; these equations were identical to Eq. (13).

Table 1: Keplerian Elements and Element Differences for LEO Test Case

	Reference Elements	Element Differences
a	7000 km	0.01 km
e	0.01	0.01
i	0.785 rad (45 deg)	0.01rad
Ω	0 rad (0 deg)	0.01 rad
ω	4.712 rad (270 deg)	0.01 rad
M_0	1.751 rad (90 deg)	0.01 rad

Figures 4-6 plot the spherical radial difference, angular cross-track, and angular along-track separations, respectively. Each figure actually contains two plots: the first shows the satellite separations described by the truth orbits and the COWPOKE approximation, and the second shows the differences between the truth and COWPOKE methods. Thus, the second plot in each figure is the error inherent in the given COWPOKE formulation.

Figure 4 shows the COWPOKE radial error to be around the 2% level. Figures 5 and 6 show the COWPOKE cross-track and along-track errors are below 1%. It is interesting to note that the radial and cross-track component errors have frequencies that appear to be once per orbit while the along-track component has an error frequency of twice per orbit. We test the COWPOKE approximations directly to determine the dominant sources of these errors.

Before continuing with the error analysis, it is useful to examine Figures 4-6 and observe the physical insight into the relative motion we can gain from the COWPOKE equations. Eq. (4) tells us that the relative motion in the radial direction is dominated by a once per orbit signature due to the eccentricity differences; the contributions from the semimajor axis difference are small, and the contribution from the true anomaly difference is an order of eccentricity smaller than the contribution from the eccentricity difference. Eq. (3) shows that the cross-track motion is comprised of once per orbit signatures from the inclination and right ascension of the ascending node differences. Eq. (13) indicates that the along-track motion is offset from zero due to the right ascension, argument of perigee, and mean anomaly differences but also has a once per orbit periodic signature with an amplitude of twice the reference eccentricity.

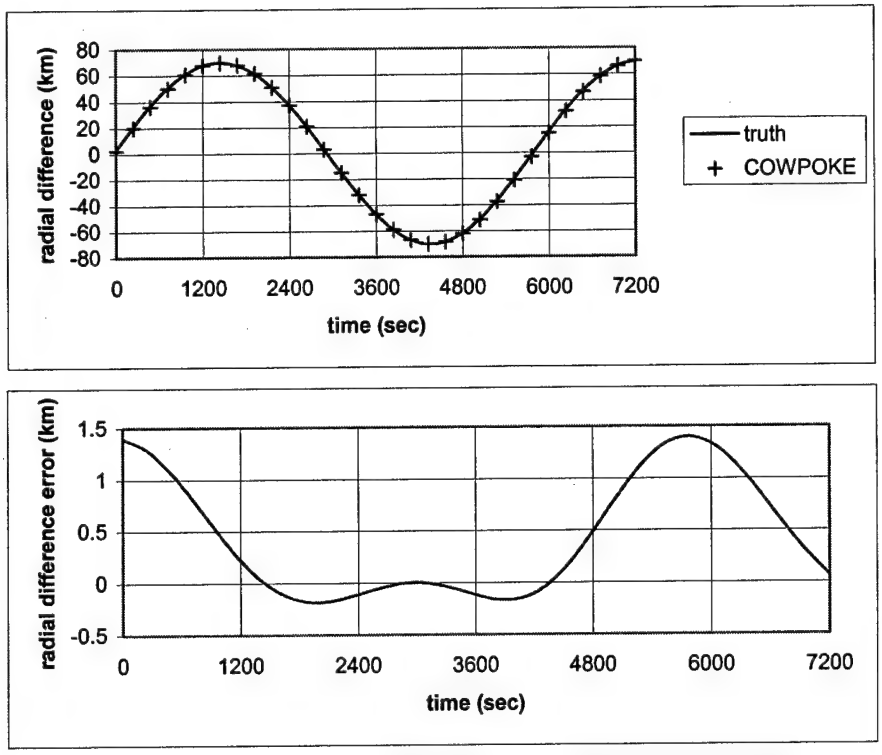

Figure 4: LEO Test Case Radial Differences and COWPOKE Errors

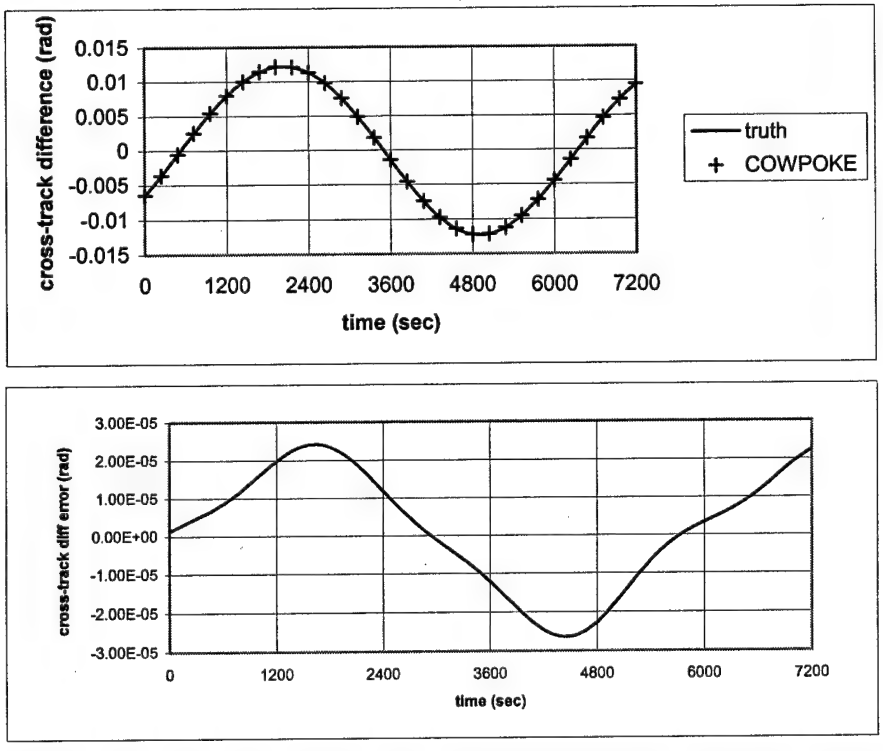

Figure 5: LEO Test Case Angular Cross-Track Differences and COWPOKE Errors

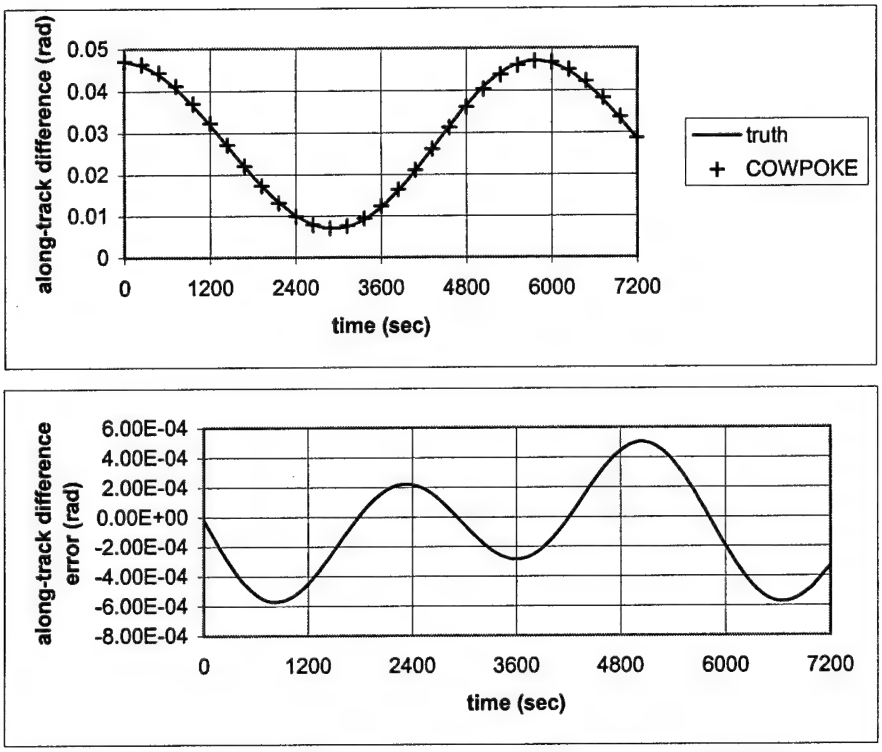

Figure 6: LEO Test Case Angular Along-Track Differences and COWPOKE Errors

Figure 7 plots the error in the first order Fourier-Bessel series expansion of the true anomaly of the reference satellite. From Figure 3, we expect to see around 1% error, and we do. Also note the twice per orbit signature in the error plot; this is also expected since the expansion only include once per orbit terms. Figure 8 plots the error in the approximation of the true anomaly difference; the error in this approximation is similar to the error in the true anomaly approximation. One sees that the dominant part of the along-track error is due to the COWPOKE approximation error of the true anomaly difference. If one chose, this error could be reduced by adding additional terms to the series approximation for this variable.

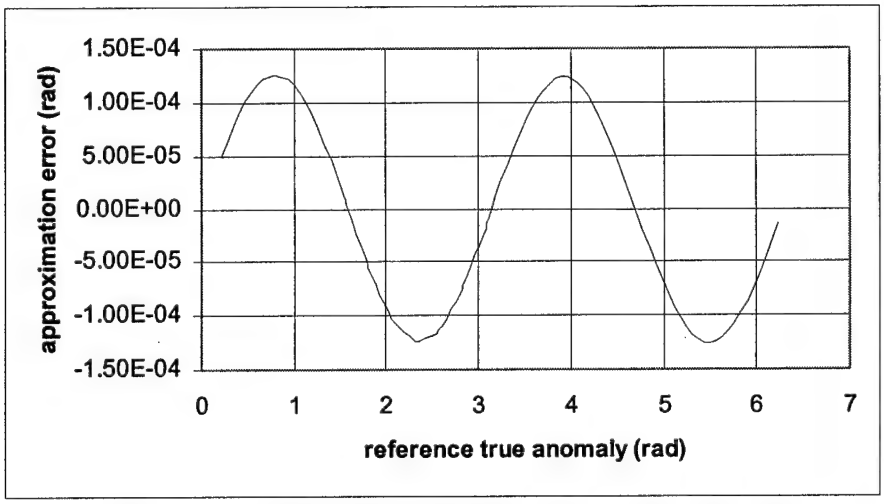

Figure 7: True Anomaly Approximation Error for LEO Test Case

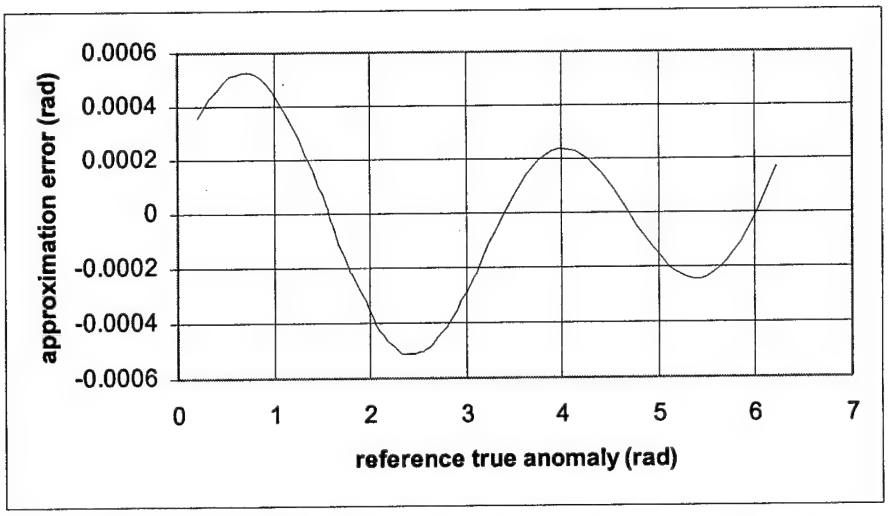

Figure 8: True Anomaly Difference Approximation Error for LEO Test Case

Figure 9 plots the errors in the COWPOKE coordinate system approximations for the LEO test case. One can see that the dominant part of the radial and cross-track errors is due to the coordinate system approximations made in the COWPOKE formulations. The radial component error can be reduced by using the analytical formulation for the radial difference while an improved description of the cross-track component would have to be derived to reduce the cross-track error.

Table 2 contains the orbital elements and element differences for the highly eccentric Earth orbit (HEO) test case. The simulation spans 12 hours or just over one orbital period. The COWPOKE formulation includes eighth order eccentricity up to frequency $6M$ and tenth order eccentricity in frequency $7M$ and $8M$; these are all of the terms included in Eqs. (8) and (10). This test case does not use the radial component approximation.

Table 2: Keplerian Elements and Element Differences for HEO Test Case

	Reference Elements	Element Differences
a	27000 km	0.01 km
e	0.7	0.01
i	0.785 rad (45 deg)	0.01rad
Ω	0 rad (0 deg)	0.01 rad
ω	4.712 rad (270 deg)	0.01 rad
M_0	1.751 rad (90 deg)	0.01 rad

Figures 10-12 plot the spherical radial difference, angular cross-track, and angular along-track separations, respectively. As with Figures 4-6, the first plot in each figure shows the satellite separations described by the truth orbits and the COWPOKE approximation, and the second plot shows the differences between the truth and COWPOKE methods. Thus, the second plot in each figure is the error inherent in the given COWPOKE formulation for this highly eccentric test case.

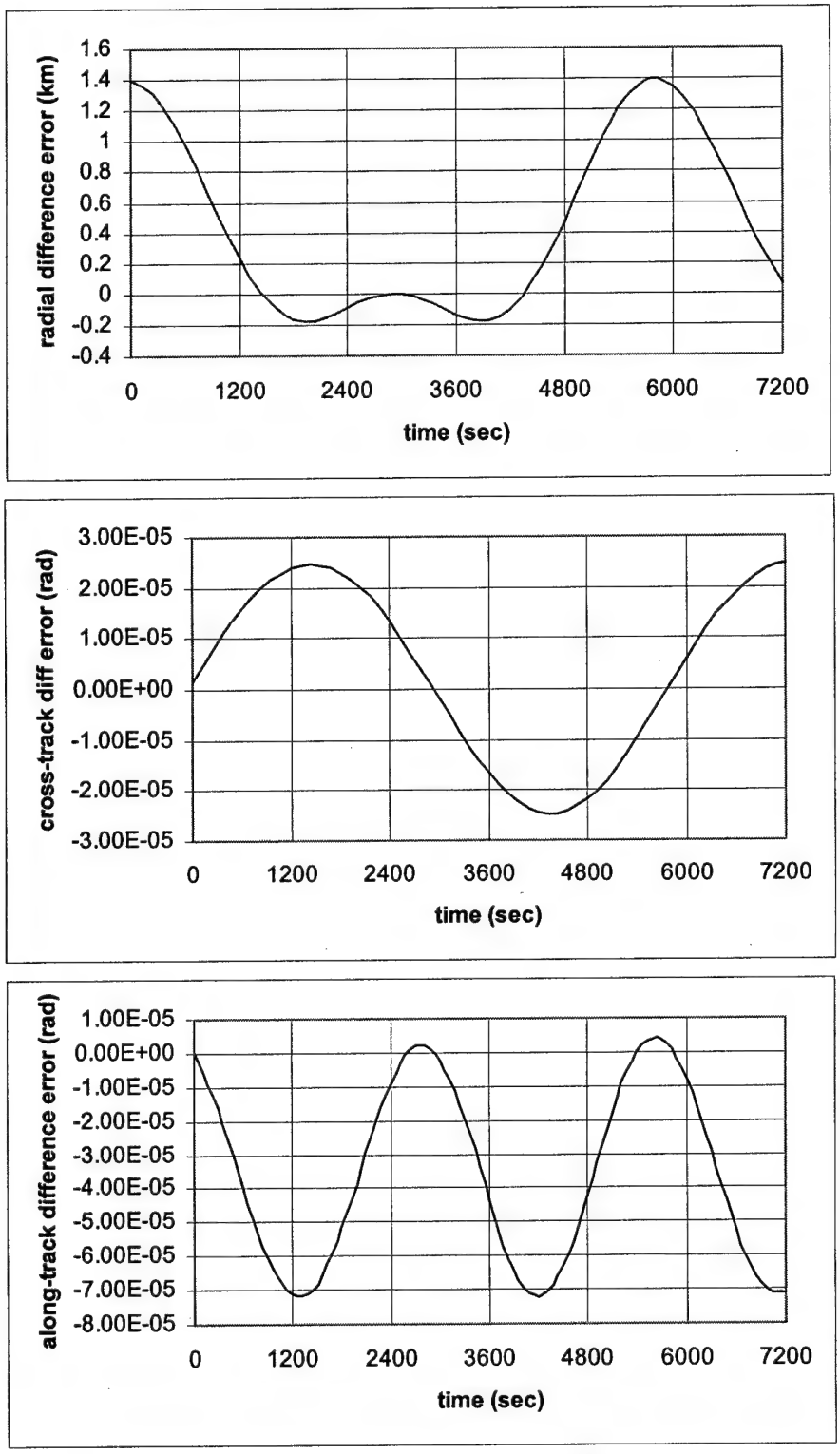

Figure 9: COWPOKE Coordinate System Approximation Errors for LEO Test Case

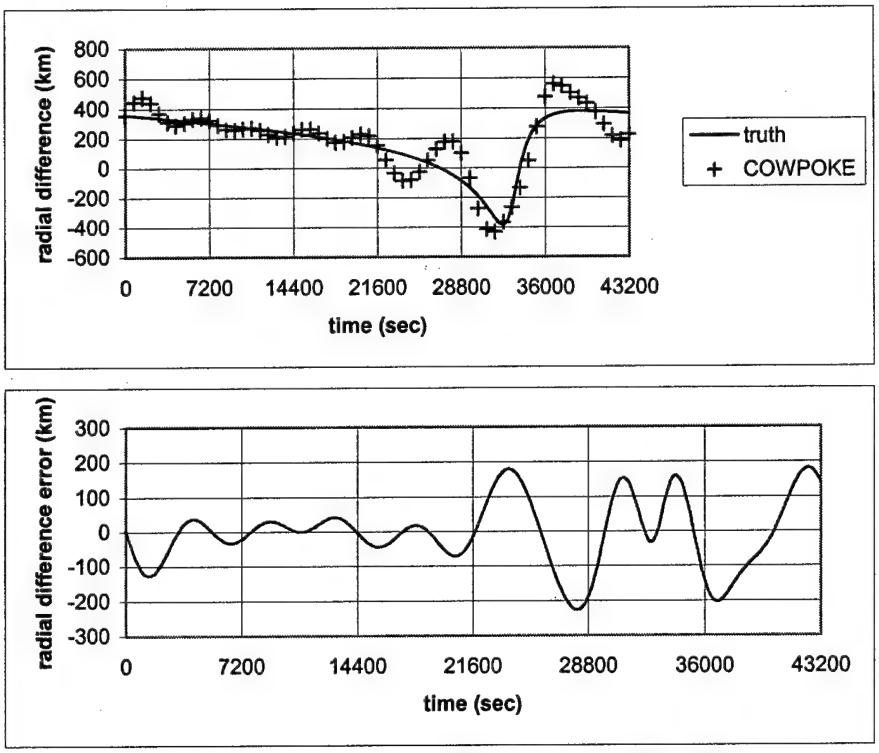

Figure 10: HEO Test Case Radial Differences and COWPOKE Errors

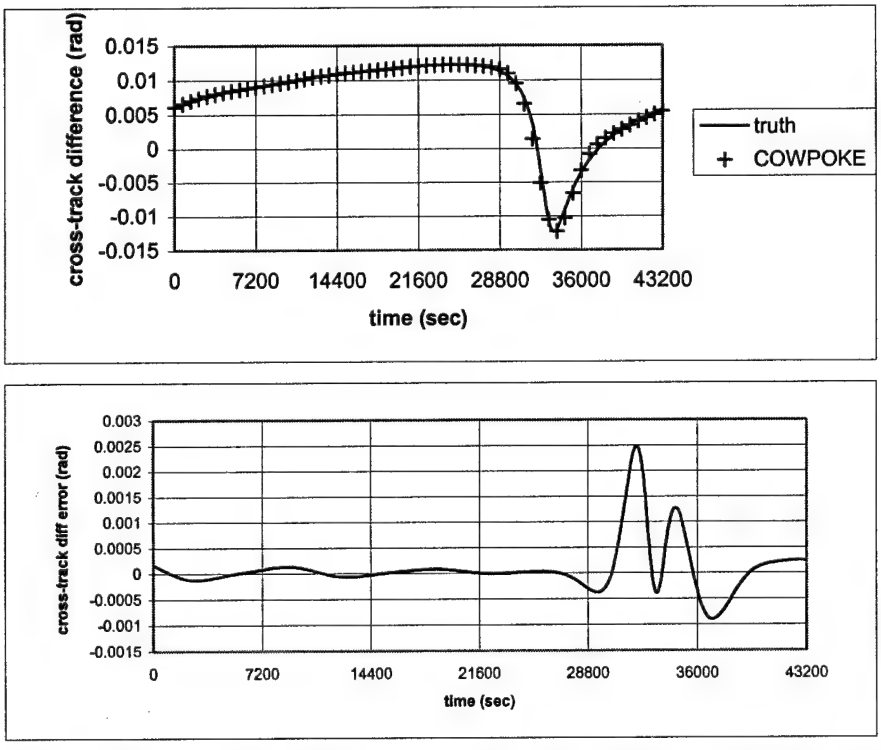

Figure 11: HEO Test Case Angular Cross-Track Differences and COWPOKE Errors

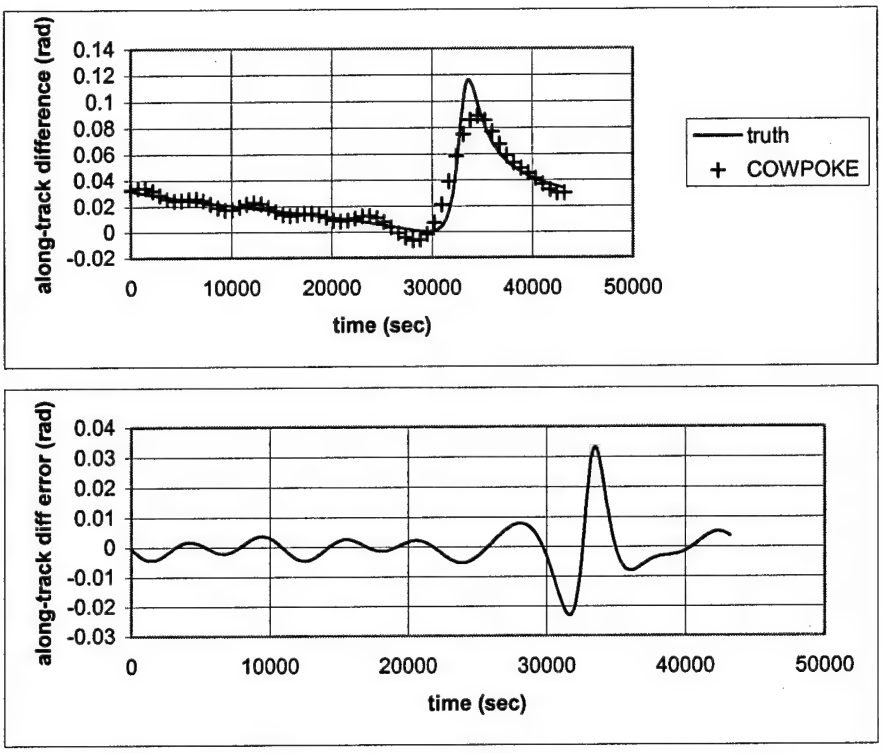

Figure 12: HEO Test Case Angular Along-Track Differences and COWPOKE Errors

Figure 10 shows the COWPOKE radial error to be significant with maximum errors being on the same order of magnitude as the relative altitude differences. Figures 11 and 12 show the COWPOKE cross-track and along-track errors are on the order of 10%. The sources of these errors can be determined by analyzing the approximations used in the COWPOKE formulation.

Figure 13 plots the error in the Fourier-Bessel series expansion of the true anomaly of the reference satellite. From Figure 3, we expect to see around 10% error, and we do along with a mixture of frequencies in the signature due to the series truncation. The error in the true anomaly approximation maps into the frequency terms and becomes the dominant source of error for the cross-track component. Figure 14 plots the error in the approximation of the true anomaly difference; the error in this approximation is an order of magnitude smaller than the error in the true anomaly approximation since we have removed an order of eccentricity in the differentiation process and replaced it by an eccentricity difference. Since the eccentricity difference is an order of magnitude smaller than the eccentricity, the eccentricity difference error is much smaller. One can see that the dominant part of the radial and along-track errors is due to the COWPOKE approximation error of the true anomaly difference and likely the eccentricity series truncation for the $8M$ frequency terms. If one chose, these errors could be reduced by adding higher order terms to the series approximations for these variables.

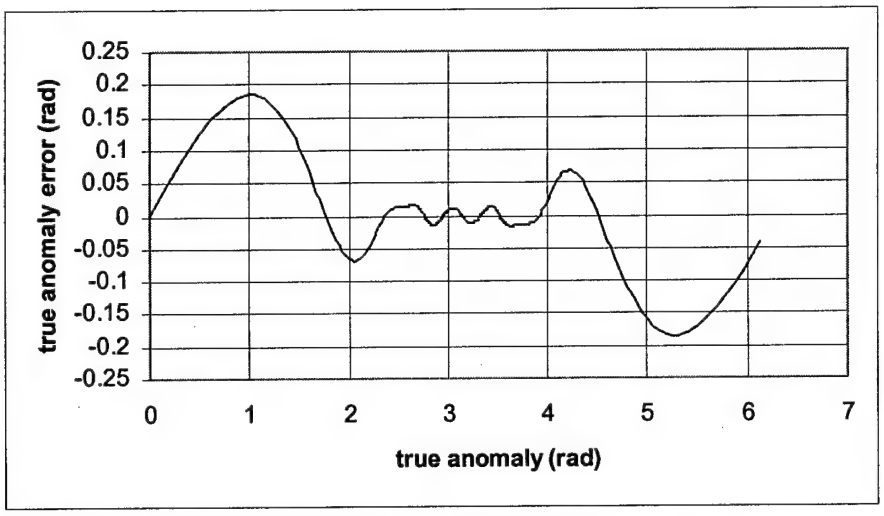

Figure 13: True Anomaly Approximation Error for HEO Test Case

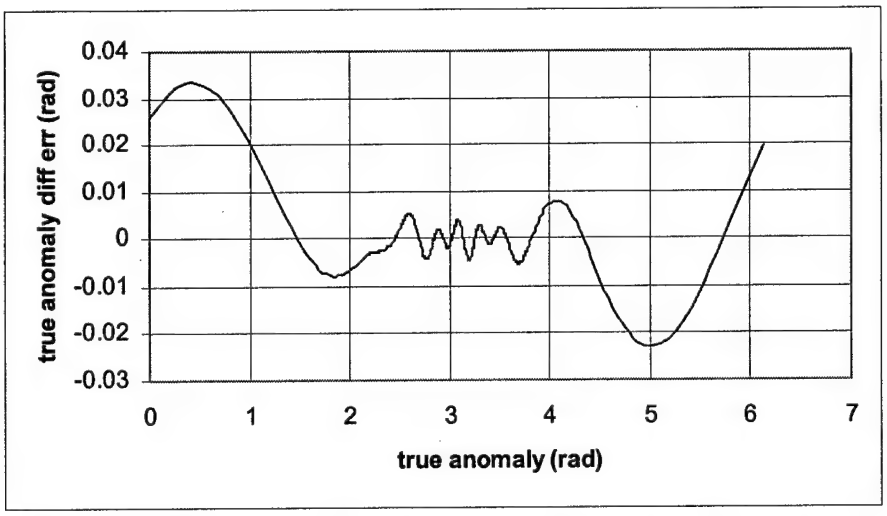

Figure 14: True Anomaly Difference Approximation Error for HEO Test Case

Figure 15 plots the errors in the COWPOKE coordinate system approximations for the HEO test case. There is no plot for the radial component since the radial approximation was not used, and thus the coordinate system error is zero. The cross-track and along-track components remain around or below the 1% level even for the high eccentricity case. It would seem that the coordinate system gives the COWPOKE equations an error bound of about 1%.

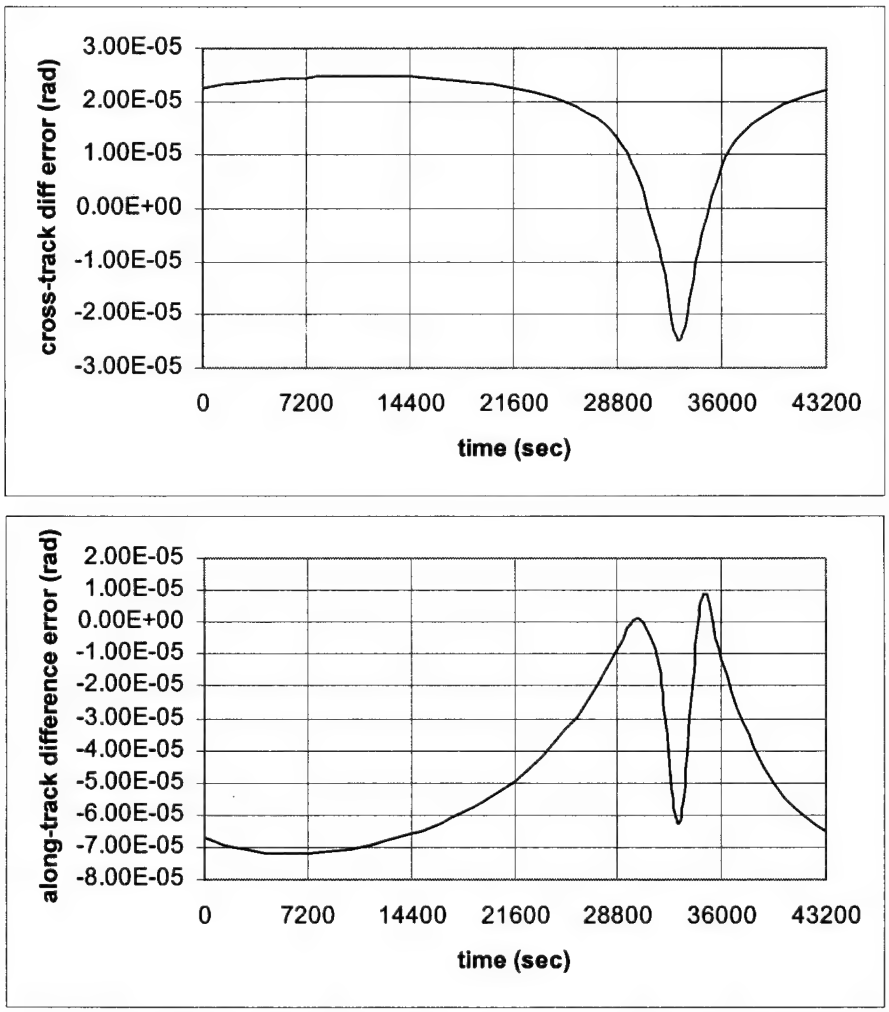

Figure 15: COWPOKE Coordinate System Approximation Errors for LEO Test Case

The cross-track and along-track errors for the HEO case are in line with expectations given the series truncations made in the COWPOKE formulation for this test case. The source of the radial error was larger than expected or desired. Further analysis of Eq. (4) shows that there is coupling between the true anomaly error and the eccentricity difference. The only way to mitigate this error is to reduce the error in the true anomaly difference approximation which can be accomplished by adding additional terms to the series expansion or by solving Kepler's equation iteratively. This would also serve to reduce the along-track errors as well.

Despite the errors present in the HEO test case, the COWPOKE equations still model bulk of the relative motion fairly well, and the geometric foundation on which the equations are built can provide a fair amount of physical insight into the relative motion. For the HEO case, the physical insight is very similar to the LEO test case except we now observe that the true anomaly does not vary linearly with time. While the series expansions do not provide a great deal of insight into how the true anomaly varies, those who are familiar with the concept should be able to anticipate the trends. In Figures 10-12, we see that as the satellite moves towards apogee (recall the initial mean anomaly was 90 deg), the true anomaly rate slows which pushes the relative motion extrema to toward the time of perigee passage. It is interesting to note that initial true anomaly difference is a function of the mean anomaly difference, eccentricity, and the initial mean anomaly; a small mean anomaly difference at perigee of a highly eccentric orbit maps into a much larger true anomaly difference than if the initial conditions occurred at apogee. Additionally, one must be aware of this fact when considering error sources in the COWPOKE formulation since only first order differences in the Keplerian elements have been included in the equations above. Finally, from the COWPOKE equations, one can see that the argument of perigee also plays a significant role in the relative motion

since the cross-track motion is dependent on both the true anomaly and the argument of perigee. The argument of perigee essentially controls the phasing between the cross-track and radial/along-track components of motion.

CONCLUSIONS AND FUTURE WORK

This paper derived the Cluster Orbits With Perturbations Of Keplerian Elements (COWPOKE) equations for unperturbed satellite motion. A general framework is provided to generate a set of equations which describe the relative motion between satellites in eccentric orbits explicitly as a function of the Keplerian elements of the reference satellite, Keplerian element differences, and time. This is accomplished using a geometric description of the separation between the satellites to form the basis of motion and then by using a Fourier-Bessel series expansion of the true anomaly in terms of the mean anomaly. True anomaly and radial differences are derived using first order perturbation methods. The resulting equations are meant to provide accurate representations of the relative motion between satellites, to be simple to implement, and to provide physical insight into the relative motion. Test cases show that this has been accomplished to a certain degree.

The geometric basis on which the COWPOKE equations are built is accurate to the 1% level when compared to the separation distances. This is currently the theoretical accuracy limitation. For most applications where the eccentricities are below 0.1, the COWPOKE equations are easily realizable and can be as accurate as the limitations of the geometric basis; however, the practical limitation for highly eccentric cases comes from generating enough terms in the series expansion of the true anomaly to reduce approximation errors to an acceptable level. This work shows that the radial component of the relative motion in our spherical reference system is particularly sensitive to true anomaly errors for high eccentricity orbits.

The next step in the development of the COWPOKE equations will be to include dynamic perturbation effects into the relative motion. Reference 8 has shown how secular effects due to Earth's oblateness can be incorporated using Keplerian elements and element differences. Simulations will also be performed to determine what other perturbations are required to support applications such as modeling geosynchronous clusters. We will also look into the invertibility of the COWPOKE equations. Here we will attempt to solve for Keplerian element differences based on desired or observed relative motion. This would be tremendously useful for formation design and geosynchronous close approach calculations.

ACKNOWLEDGMENTS

This research is sponsored by the Air Force Office of Scientific Research (AFOSR). The authors would like to thank Maj. William Hilbun of the Computational Mathematics Division and Dr. Clifford Rhoades of the Mathematics and Space Sciences Directorate of AFOSR for their support and commitment to basic research at the AMOS site. The authors would like to acknowledge the contributions of Dr. Chuck Matson, Mr. Paul Kervin, Lt. Col. Jeff McCann, Ms. Valerie Skarupa, Capt. Dale White, and Dr. Joseph Janni in building and maintaining the AMOS basic research program. Finally, we would like to thank Rich Burns, now with the NASA Goddard Space Flight Center, for his previous contributions to AFRL formation flying efforts and Terry Alfriend of Texas A&M University for his useful comments over the last several years.

REFERENCES

1. Abbot, R., R. Clouser, E. Evans, J. Sharma, "Close Geostationary Satellite Encounter Analysis: 1997-2001," presented at the AAS/AIAA Space Flight Mechanics Meeting, San Antonio, TX, 27-30 January 2002, AAS 02-115.
2. Hill, G. W., "Researches in the Lunar Theory," *American Journal of Mathematics*, Vol. 1, No. 1, 1878, pp. 5-26.
3. Clohessy, W. H., R. S. Wiltshire, "Terminal Guidance System for Satellite Rendezvous," *Journal of the Aerospace Sciences,* September 1960, pp. 653-658
4. Gim, D., K. Alfriend, "The State Transition Matrix of Relative Motion for the Perturbed Non-Circular Reference Orbit," presented at the AAS/AIAA Space Flight Mechanics Meeting, Santa Barbara, CA, 11-15 February 2001, AAS 01-222.
5. Garrison, J. L., T. G. Gardner, P. Axelrad, "Relative Motion in Highly Elliptical Orbits," *Advances in the Astronautical Sciences,* Vol. 89, No. 1, 1998, pp. 148-155.
6. Melton, R. G., "Time-Explicit Representation of Relative Motion Between Elliptical Orbits," *Journal of Guidance, Control, and Dynamics,* Vol. 23, No. 4, July-August 2000, pp. 604-610.
7. Sabol, C., R. Burns, C. McLaughlin, "Satellite Formation Flying Design and Evolution," *Journal of Spacecraft and Rockets*, Vol. 38, No. 2, March-April 2001, pp. 270-278.
8. McLaughlin, C., R. Burns, C. Sabol, K. Luu, "Modeling Relative Position, Relative Velocity, and Range Rate for Formation Flying," presented at the AAS/AIAA Astrodynamics Conference, Quebec City, Canada, 30 July - 2 August 2001, AAS 01-457.
9. Swank, A., C. McLaughlin, C. Sabol, R. Burns, "Long Duration Analysis of the J2-Model Equations of Relative Motion for Satellite Clusters," presented at the AAS/AIAA Space Flight Mechanics Meeting, San Antonio, TX, 27-30 January 2002, AAS 02-185.
10. Battin, R. H., *An Introduction to the Mathematics and Methods of Astrodynamics,* AIAA Education Series, 1987, AIAA, Washington DC.
11. Vallado, D. A., *Fundamentals of Astrodynamics and Applications*, McGraw-Hill, New York, 1997
12. Baoyin, H., L. Junfeng, G. Yunfeng, "Dynamical behaviors and relative trajectories of the spacecraft formation flying," *Aerospace Science and Technology*, Vol. 6, 2002, pp. 295-301

RELATIVE ORBIT DETERMINATION OF GEOSYNCHRONOUS SATELLITES USING THE COWPOKE EQUATIONS

Keric Hill
University of Colorado, Boulder, CO 90309

Chris Sabol, K. Kim Luu
AMOS (AFRL), 535 Lipoa Pkwy Ste 200, Kihei, HI 96753

Michael Murai
AMOS (Oceanit), 590 Lipoa Pkwy Ste 264, Kihei, HI 96753

Craig McLaughlin
University of North Dakota Grand Forks, ND 58202

ABSTRACT

Optical satellite tracking often reveals multiple satellites in a single telescope field of view. The Cluster Orbits With Perturbations Of Keplerian Elements (COWPOKE) equations are used to estimate the relative motion of geosynchronous satellites and determine if the satellites can be later identified based solely on relative position. This paper provides the development of the COWPOKE equations for modeling the relative motion of geosynchronous satellites and analysis demonstrating the feasibility of using these techniques for object correlation. Real data relative orbit determination results are provided using the optical tracking assets of the Air Force Maui Optical and Supercomputing (AMOS) site.

1. INTRODUCTION

Clusters of spacecraft in geosynchronous orbit (GEO) are becoming more common. Orbital slot allocations in GEO are rapidly being filled, and it is increasingly difficult to acquire slots for new satellites. Consequently, many organizations opt to collocate their spacecraft in the same slot. Eutelsat had as many as five satellites collocated in a formation at 13° E by 2001 [i]. In addition, unintentional close approaches have occurred and could become more frequent as the GEO belt becomes more crowded. In 1997, Telstar 401, a satellite in GEO, experienced a major failure, and control of the spacecraft was lost [ii]. It is drifting in GEO and has had encounters with other satellites as close as 4 km [iii]. Since that time, other GEO spacecraft have also begun drifting uncontrollably. Close approaches and satellite formations create a challenge for space surveillance. Identification of the satellites in these clusters can be difficult, and cross-tagging (misidentification) occurs [iv]. Resolvable imaging can be used to identify spacecraft in low Earth orbit but is not currently possible for GEO altitudes. Non-imaging approaches include comparing the brightness and characterizing the color of light reflected from the spacecraft for identification purposes [v]. However, identifying spacecraft solely from their dynamics would eliminate the need for special filters or other sensors. A better understanding of the relative motion of the spacecraft could reduce cross-tagging and improve close approach predictions. Improved determination of minimum approach distances could eliminate unnecessary collision avoidance maneuvers and minimize propellant usage.

Cluster orbits can be modeled using the Cluster Orbits With Perturbations Of Keplerian Elements (COWPOKE) equations of motion [vi]. The COWPOKE equations predict spacecraft separations in the spherical radial, along-track, and cross-track coordinate frame based on the Keplerian elements of the reference satellite, the element differences for the second satellite, and elapsed time. These inputs for COWPOKE can be obtained with relative metric data from optical sensors or space surveillance products. Charge-coupled device (CCD) images of clusters of spacecraft should provide very accurate measurements of spacecraft separation since in-frame error sources theoretically cancel out. The United States Air Force currently operates several optical systems capable of imaging clusters at the Maui Space Surveillance Complex, such as Raven, Phoenix, and the Ground-Based Electro-Optical Deep Space Surveillance System (GEODSS). Raven uses small, commercially available telescopes to acquire CCD images of space objects for tracking [vii]. Astrometry is used to match stars in the CCD image to the star catalog. Thus, the pointing accuracy of the images can approach the accuracy of the star catalog used. Phoenix is a Baker-Nunn telescope refurbished to take wide-angle CCD images [viii]. As many as 21 satellites have been detected in one Phoenix image. After the Deep Stare upgrade, GEODSS could be used to acquire relative metrics as well.

This paper is an extension of previous work exploring the application of COWPOKE towards geosynchronous cluster orbit prediction [ix]. First, a perturbation study is conducted to determine the force modeling required at GEO. Improvements are made to the COWPOKE equations that allow for better representation of GEO motion. A method is construed to estimate the Keplerian element differences using optical measurements of relative right ascension and declination. Finally, results are discussed for which COWPOKE was used to predict the relative motion of a cluster of satellites in GEO.

2. USING COWPOKE AT GEO

A study was conducted to identify perturbing forces that significantly affect the relative motion of a cluster of geosynchronous satellites. The effects of central body gravity, third body gravity, and solar radiation pressure were investigated using the Draper Semianalytic Satellite Theory (DSST). The Draper research and development version of the Goddard Trajectory Determination System (DGTDS) was used to propagate the orbits with DSST [x]. The motion of two spacecraft was propagated to generate a "truth" relative motion using an 8x8 JGM-2 geopotential field, luni-solar third-body point-mass using JPL ephemerides, and solar radiation pressure (SRP) based on a spherical satellite and cylindrical Earth-shadow model. Next, the relative motion of the two spacecraft was generated while neglecting one of the sources of perturbations, such as third-body gravity. The radial, along-track, and cross-track separations obtained from the "truth" relative motion were compared to those generated with the incomplete force model to find the approximate error that would result from neglecting that perturbation source in the COWPOKE formulation. These test runs were conducted two times; the first set of runs included long period effects propagated over 30 days, and the second set investigated short periodic effects propagated over 5 days. Table 1 shows the reference elements and the differential elements used in the propagation.

Table 1. Initial conditions for DSST runs referenced to the mean equator and equinox of the B1950.0 coordinate system.

Keplerian Elements	Reference Elements	Element Differences
a	42,164 km	0
e	0.01	0.01
i	3°	1°
Ω	0°	1°
ω	0°	1°
M_0	0°	1°

Cases that neglected all non-spherical gravity forces were conducted at differing initial mean anomalies. Those omitting higher order geopotential terms, but including J_2, were conducted with varying longitudes of the node to survey the longitudinal dependencies of the tesseral harmonics. Tests examining luni-solar effects ran at varying days of the year while those for SRP effects used different days of the year as well as at various differential area-to-mass ratios for the spacecraft. Errors were calculated by dividing the difference in radial, along-track, or cross-track separation by the maximum separations. Fig. 1 shows the worst case errors produced by neglecting each of the perturbing forces after 30 days.

The SRP results in Fig. 1 arise from a case in which the area-to-mass ratio of one satellite is ten times that of the other. As the separation between the spacecraft decreases to zero, the effect of neglecting gravitational effects also decreases to zero; however, SRP effects do not decrease to zero if the area-to-mass ratios differ. Because of this, SRP effects should be taken into account if high accuracy is warranted over long periods or if the satellites are within several kilometers.

The effects of SRP on an orbit were formulated using Keplerian elements and the element differences, assuming that the latter quantities are small. However, because Keplerian elements are singular for $i = 0$ and $e = 0$, orbits in GEO can have large differences in Ω, ω, and M_0 and still remain within a few kilometers of each other. Simulations found that this formulation of SRP did not prove to be useful for GEO and therefore was not used in later tests. However, for most cases, two-body motion results in acceptably low error.

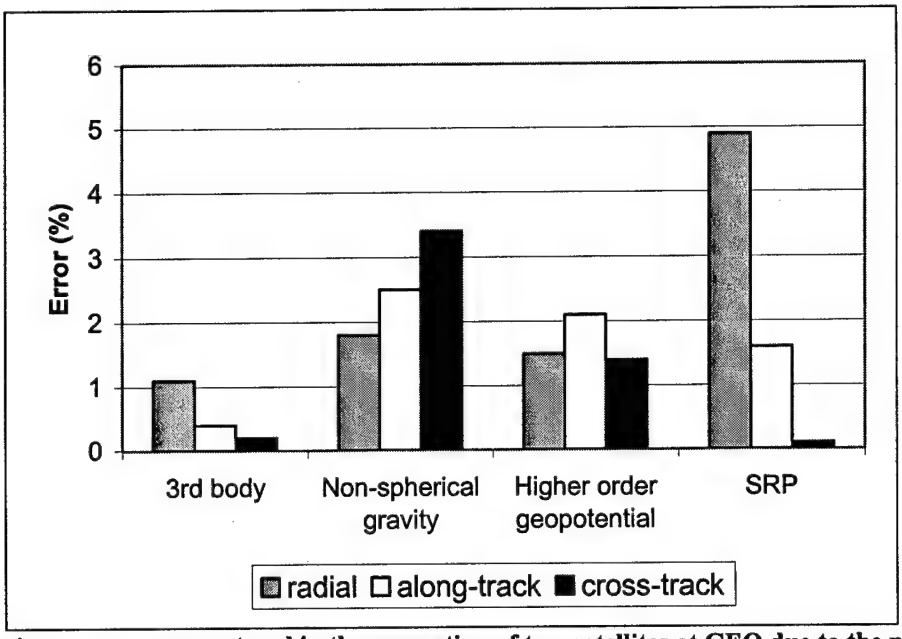

Fig. 1. Maximum error encountered in the separation of two satellites at GEO due to the neglect of a perturbing force after a 30-day orbit propagation.

Another source of orbit perturbation is stationkeeping and momentum control maneuvers. Since maneuvers were not modeled in COWPOKE, they present an additional source of error if occurring during the observation period.

3. IMPROVED COWPOKE EQUATIONS

Although COWPOKE has been shown to be an effective predictor of the relative motion of a cluster of satellites, there are some sources of error. For GEO, the right ascension of the ascending node, argument of perigee, and mean anomaly element differences may not be small which violates the assumptions of the original COWPOKE derivation. In particular, the approximation of the true anomaly difference was linear in terms of the mean anomaly difference; this causes error, particularly in the along-track direction, when the mean anomaly difference is significant. The cross-track term component of COWPOKE also showed error with large right ascension differences.

Replacing the linear approximation of the true anomaly difference with an exact difference of the two true anomaly terms substantially reduced the along-track error. For the near-circular GEO case, the true anomaly of each satellite as a function of time is approximated by a first order expansion in terms of eccentricity and mean anomaly which was shown to be effective in [6]. The cross-track component was improved by an investigation into the spherical geometry involved. Corrections were made to both amplitude and phasing of the cross-track component which are accurate for large values of right ascension of the ascending node, argument of perigee, and mean anomaly differences. The improved COWPOKE equations are

$$
\begin{aligned}
\delta r &= \frac{(a+\delta a)\left(1-(e+\delta e)^2\right)}{1+(e+\delta e)\cos\left(M+2e\sin(M)+\delta\upsilon\right)} - \frac{a\left(1-e^2\right)}{1+e\cos(\upsilon)} \\
\frac{\delta xt}{r} &= -2\sin\left(\frac{\delta\Omega}{2}\right)\sin(i)\cos\left(\omega+\frac{\delta\omega}{2}+M+2e\sin(M)+\frac{\delta\upsilon}{2}\right) \\
&\quad + \delta i\sin\left(\omega+\delta\omega+M+2e\sin(M)+\delta\upsilon\right) \\
\frac{\delta at}{r} &= (\delta\omega+\delta\upsilon)\cos(\delta i)+\delta\Omega\cos(i)
\end{aligned}
\tag{1}
$$

where

$$\delta M = \delta M_0 + \left(\sqrt{\frac{\mu}{(a+\delta a)^3}} - \sqrt{\frac{\mu}{a^3}} \right) t$$
$$\delta v = \delta M + 2(e+\delta e)\sin(M+\delta M) - 2e\sin(M) \tag{2}$$

δr is the separation in the radial direction, δxt is the cross-track separation, and δat is the along-track separation. δv is the difference in true anomaly. a, e, i, Ω, ω, and M are the orbital elements of the reference satellite, and δa, δe, δi, $\delta\Omega$, $\delta\omega$, and δM are the differences in the elements of the two satellites. μ is the gravitational parameter, and t is the time elapsed since the epoch of M.

The along-track term still exhibits error when the δΩ and δi terms are large. To avoid this as an error source in the relative orbit determination experiments, it was decided to use the along-track component from Vadali's unit sphere model for relative motion [xi]. The Vadali unit sphere model is very similar in philosophy to COWPOKE; relative motion is modeled through Keplerian elements and element differences. Vadali's geometric model, however, is more rigorous than the simple COWPOKE approach. Here is the along-track component of Vadali's unit sphere model which was incorporated into COWPOKE for the remainder of this analysis:

$$\begin{aligned}
\frac{\delta at}{r} = {} & \cos^2(i/2)\cos^2((i+\delta i)/2)\sin(\delta\omega+\delta v+\delta\Omega) \\
& + \sin^2(i/2)\sin^2((i+\delta i)/2)\sin(\delta\omega+\delta v-\delta\Omega) \\
& - \sin^2(i/2)\cos^2((i+\delta i)/2)\sin(2(\omega+v)+\delta\omega+\delta v+\delta\Omega) \\
& - \cos^2(i/2)\sin^2((i+\delta i)/2)\cos(2(\omega+v)+\delta\omega+\delta v-\delta\Omega) \\
& + \frac{1}{2}\sin(i)\sin(i+\delta i)\left[\sin(\delta\omega+\delta v)+\sin(2(\omega+v)+\delta\omega+\delta v)\right]
\end{aligned} \tag{3}$$

4. DETERMINATION OF ELEMENT DIFFERENCES

Predicting the relative motion of a cluster of satellites with COWPOKE requires a set of orbital elements for the reference satellite and the relative elements of the second satellite. A least-squares orbit determination method was used to find these element differences [xii].

COWPOKE expresses spacecraft separations in the spherical radial, along-track and cross-track reference frame, but the optical observations used in this effort are in the topocentric right ascension and declination frame. Therefore, the topocentric observations had to be converted to geocentric observations, which requires satellite range knowledge as well as the local sidereal time [xiii]. For this analysis, a constant range value was used and values of UT1-UTC, precession and nutation angles, and lunar terms were ignored; it is believed that these approximations do not have significant impact once the observations are differenced. The COWPOKE cross-track and along-track separations could then be equated with the geocentric right ascension and declination frame as follows:

$$\begin{aligned}
\delta\alpha &= \delta at\cos\theta - \delta xt\sin\theta \\
\delta d &= \delta xt\cos\theta + \delta at\sin\theta
\end{aligned} \tag{4}$$

where

$$\theta = i\cos(\omega+\upsilon) \tag{5}$$

Let Y be the relative observation vector, and X the state vector containing the orbital element differences. Eqs. (4) & (5) represent a nonlinear mapping between the state vector and the observations. In order to invert the problem, we must linearize the equations about a reference trajectory, X^*.

$$Y = \begin{bmatrix} \delta\alpha \\ \delta d \end{bmatrix} = F(X) \approx F(X^*) + \left.\frac{\partial F}{\partial X}\right|_{X^*} (X - X^*) \tag{6}$$

$$X = \begin{bmatrix} \delta a & \delta e & \delta i & \delta\Omega & \delta\omega & \delta M_0 \end{bmatrix}^T \tag{7}$$

The $\delta\alpha$ terms are the observed differences in right ascension, and the δd are the observed differences in declination. Eq. (6) can be rearranged and terms can be redefined as follows:

$$\begin{aligned} Y - F(X^*) &\approx \left.\frac{\partial F}{\partial X}\right|_{X^*} (X - X^*) \\ y &= Hx \end{aligned} \tag{8}$$

where y is the difference between the observed and calculated relative observations, H is the linearized observation-state relationship, and x is the estimated correction to the state matrix. If at least 3 relative observation pairs are included in the y vector, one can estimate the state deviation as shown below:

$$x = \left(H^T H\right)^{-1} H^T y \tag{9}$$

The estimate of the state can be updated in an iterative fashion, as shown below, until the solution converges.

$$X^*_{i+1} = X^*_i + x \tag{10}$$

Using this method, an estimate of the Keplerian element differences was obtained. This method requires that the Keplerian elements of the reference satellite are known. The NORAD two-line element set (TLE) of the reference satellite was used for the reference orbit in this study. With the element differences, the relative right ascension and declination of the two satellites can be predicted using COWPOKE.

5. SIMULATION STUDY

In order to test the feasibility of using COWPOKE to better predict relative motion, a simulation was performed using 2 collocated geosynchronous satellites. Truth orbits were propagated using the Cowell Special Perturbations (SP) propagator internal to DGTDS. The truth orbits spanned from Jan 1 – Feb 5, 2003. Table 2 contains the osculating orbital elements for the satellites referenced to the mean equator and mean equinox of the B1950.0 coordinate system.

Table 2. The initial orbital elements of the two satellites used in the identification study with epoch January 1, 2003, 0 hr.

	Satellite1	Satellite2
Semimajor Axis (km)	42164	42164
Eccentricity	0.000512	0.000812
Inclination (deg)	0.05	0.05
Right Ascension of the Ascending Node (deg)	20	340
Argument of Perigee (deg)	33	67
Mean Anomaly (deg)	0	6

The next step in the process was to develop TLE representations of the truth orbits. This step was necessary since TLEs are used in the observation correlation process. To do this, an orbit using the GP4/DP4 propagator internal to DGTDS was fit to the position and velocity vectors produced by the Cowell truth trajectory. The position and

velocity data spanned 1 Jan to 1 Feb and were spaced at every hour. The resulting fits were accurate to around the 2 km level RMS. Fig. 2 plots the DP4 trajectories relative to the truth orbit of Sat 1 over February 1-5, a 5-day prediction interval.

One can clearly see in Fig. 2 that the TLE trajectory for Sat 2 comes closer to the Truth location for Sat 1 than the Truth location for Sat 2 during a significant portion of the orbit. Similarly, the TLE trajectory for Sat 1 comes close to the Truth location for Sat 2 during a portion of the orbit. Both of these situations could lead to a cross-tag in the observation correlation process (i.e., observations of Sat 2 could be incorrectly attributed to Sat 1 and vice versa).

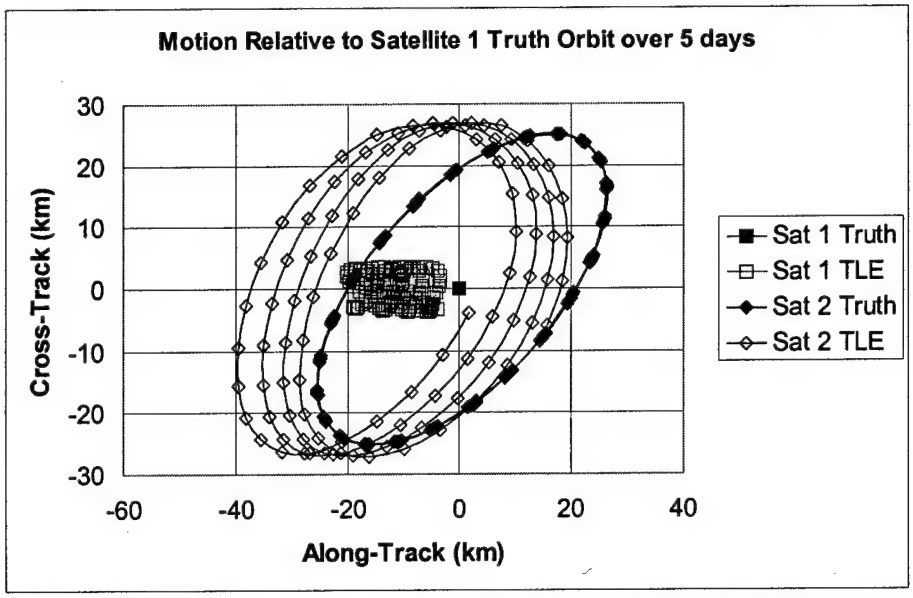

Fig. 2. TLE orbit predictions of the motion of Satellite 2 relative to Satellite 1 truth orbit compared to the truth relative motion.

The mean orbital elements from the TLE fits (epoch 1 Feb) were differenced and used to initialize the COWPOKE equations along with the TLE elements for Sat 1. One can see in Fig. 3 that even using the flawed initial conditions produced by the TLE fits, the relative motion is very representative of the Truth relative motion. This signifies that the relative position is a powerful piece of information that can be used to help correlate optical observations at the sensor.

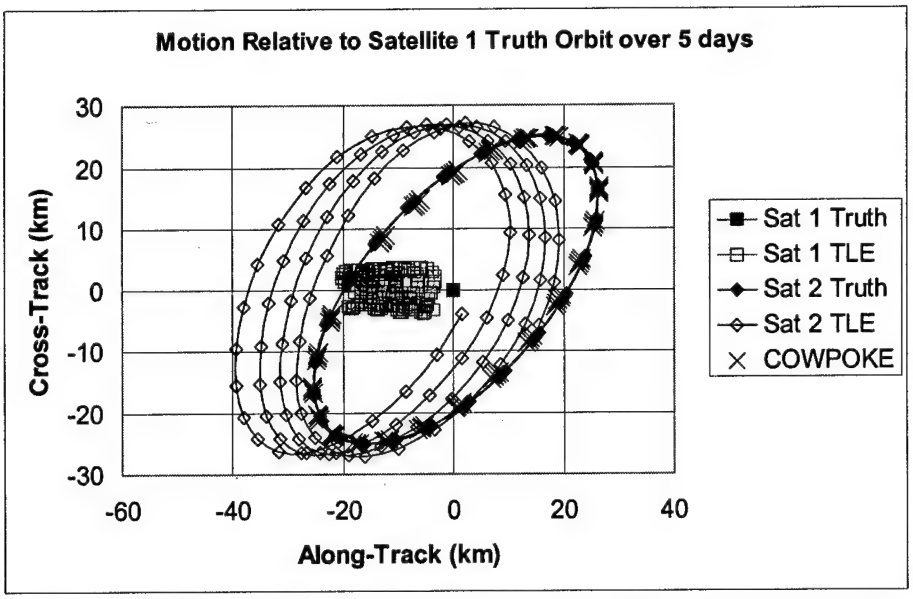

Fig. 3. COWPOKE relative motion predictions with TLE and truth orbits.

6. REAL DATA RESULTS

Observations from Raven were used to test COWPOKE's effectiveness. Raven images were taken of the DirecTV 4S and AMC 4 spacecraft collocated at 101° West longitude during the nights of July 23-24 and July 29-August 1, 2003. One of these images is shown in Fig. 4.

Raven images were used to compute the separation of the two satellites. Sat 1, the reference satellite, was chosen to be AMC-4, and DirecTV 4S was designated Sat 2. The reference orbit for Sat 1 was generated using the TLE from July 20, 2003. Other TLEs might be available at an epoch closer to the 24th, but for R&D Raven operations, the catalog is only updated every few days. The observed separation in right ascension and declination on the night of the 23rd were used to estimate the Keplerian element differences. The observations from the 23rd didn't span a long enough period to accurately solve for the difference in semimajor axis, so an *a priori* estimate of 0 m was added for δa, with a standard deviation of 1000 km. With the resulting estimate of the element differences, COWPOKE was used to predict the relative position of the two satellites at the time of each observation taken on the night of the 24th. The COWPOKE predictions are compared to the positions predicted by the TLEs at the time of each observation in Fig. 5. The COWPOKE prediction of the location of Sat 2 was off by an average of 155 microradians, while the TLE predictions differed from the observations by an average of 576 microradians.

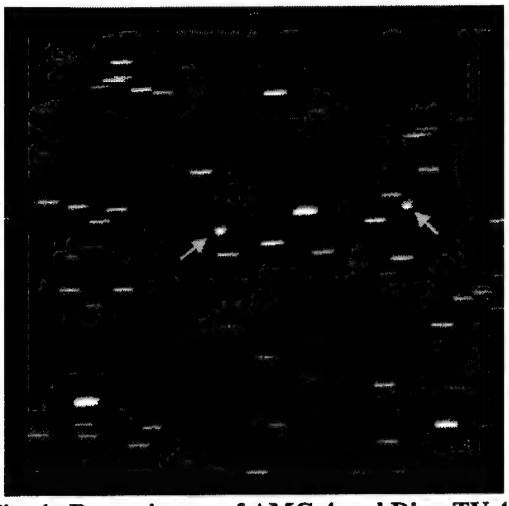

Fig. 4. Raven image of AMC-4 and DirecTV 4S

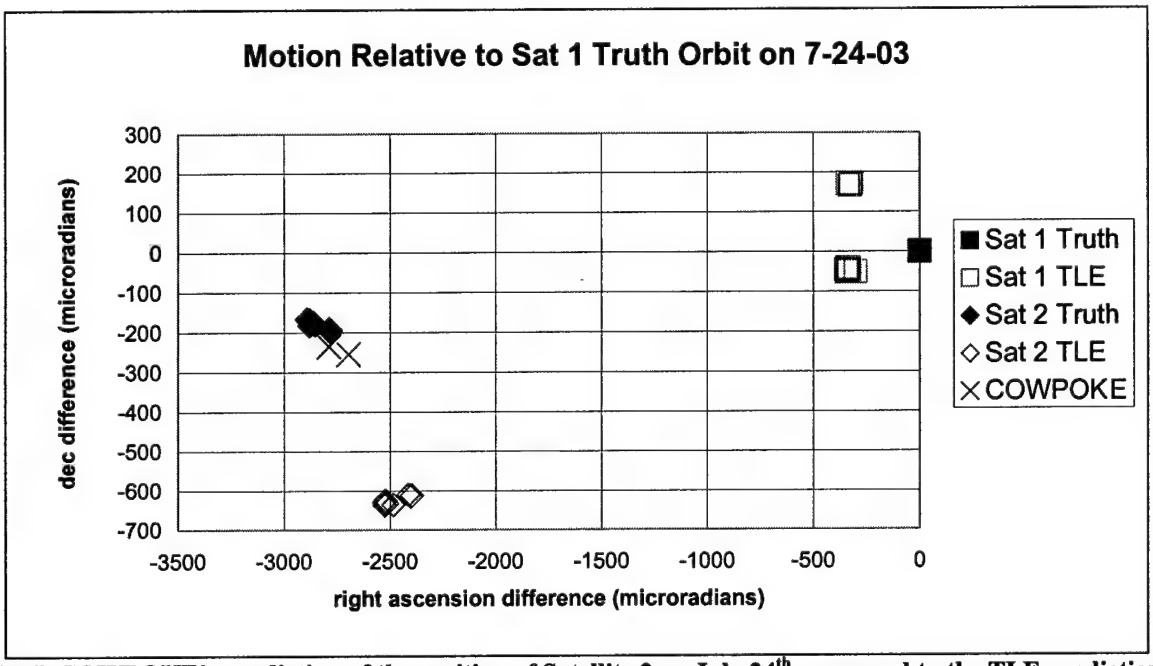

Fig. 5. COWPOKE's prediction of the position of Satellite 2 on July 24th compared to the TLE predictions

The observations from July 23 and 24 were used to estimate the element differences and predict the relative motion for July 29, when the next telescope images were taken. DP4 predictions and the COWPOKE reference orbit were obtained using TLEs for Sat 1 and Sat 2 from the 26th and 27th respectively. The results for the 29th are shown in Fig. 6. The COWPOKE predictions differed from the truth by an average of 390 microradians, while the TLE predictions were off by 721 microradians.

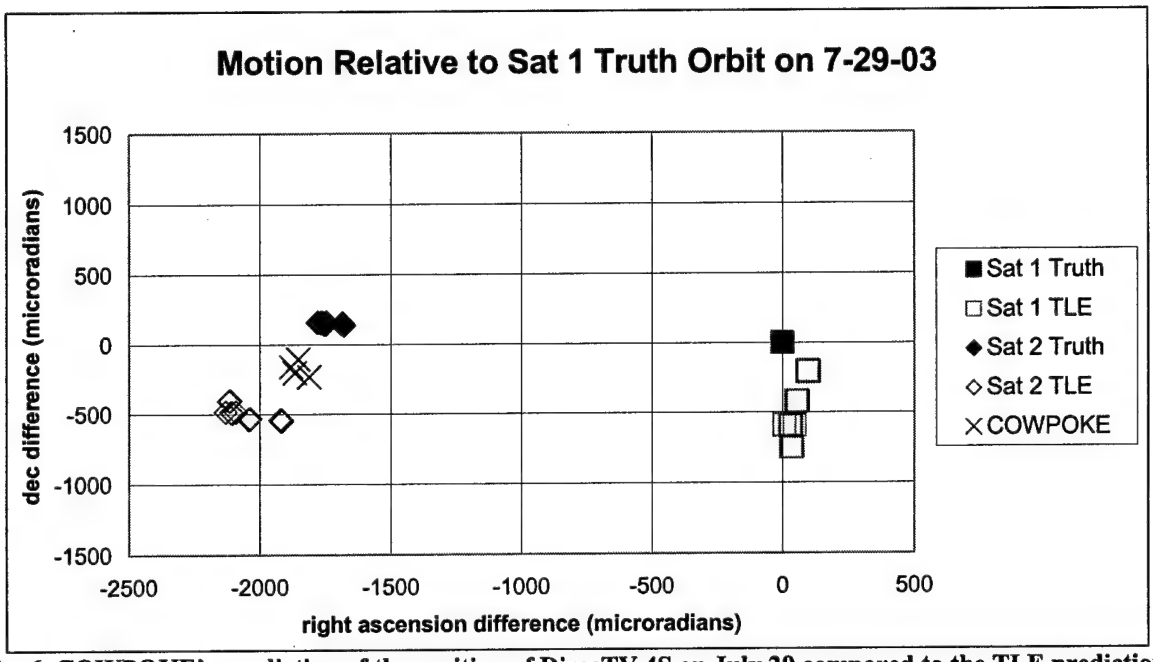

Fig. 6. COWPOKE's prediction of the position of DirecTV 4S on July 29 compared to the TLE predictions

The observations from July 23, 24, and 29 were then used to estimate improved element differences. Those element differences were used to predict the relative position of Sat 2 on the 30th, and the results are plotted in Fig. 7. COWPOKE had an average error of 300 microradians, and the TLE for Sat 2 averaged 894 microradians. Fig. 8 shows the results of similar predictions for July 31 using the observations from all previous nights. To be clear, the TLE prediction span at this point is several days while the COWPOKE prediction is only one day.

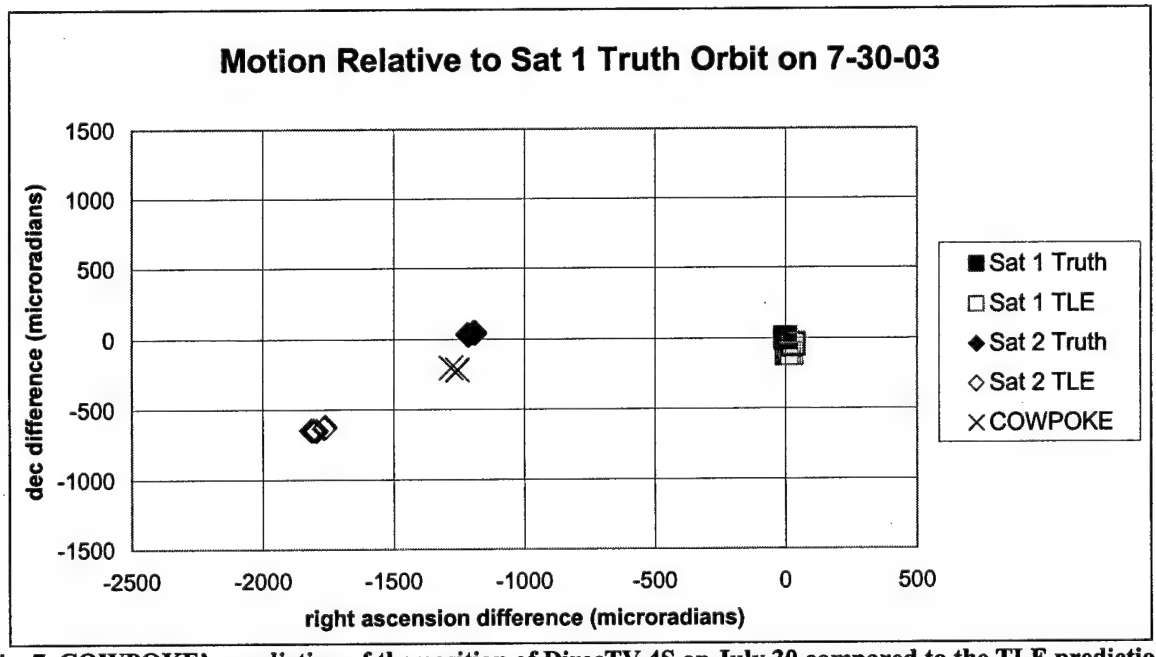

Fig. 7. COWPOKE's prediction of the position of DirecTV 4S on July 30 compared to the TLE predictions

In Fig. 8, one can see that the true position of Sat 1 has shifted away from the TLE prediction since the night before. Also, the COWPOKE prediction no longer matches the observation for Sat 2, especially in declination. There is strong evidence that Sat 1 performed a stationkeeping maneuver between the 30th and the 31st. Even with the

possible maneuver, COWPOKE still provided a better estimate of the relative motion than the TLE. COWPOKE had an average error of 450 microradians, and TLE for Sat 2 averaged 869 microradians.

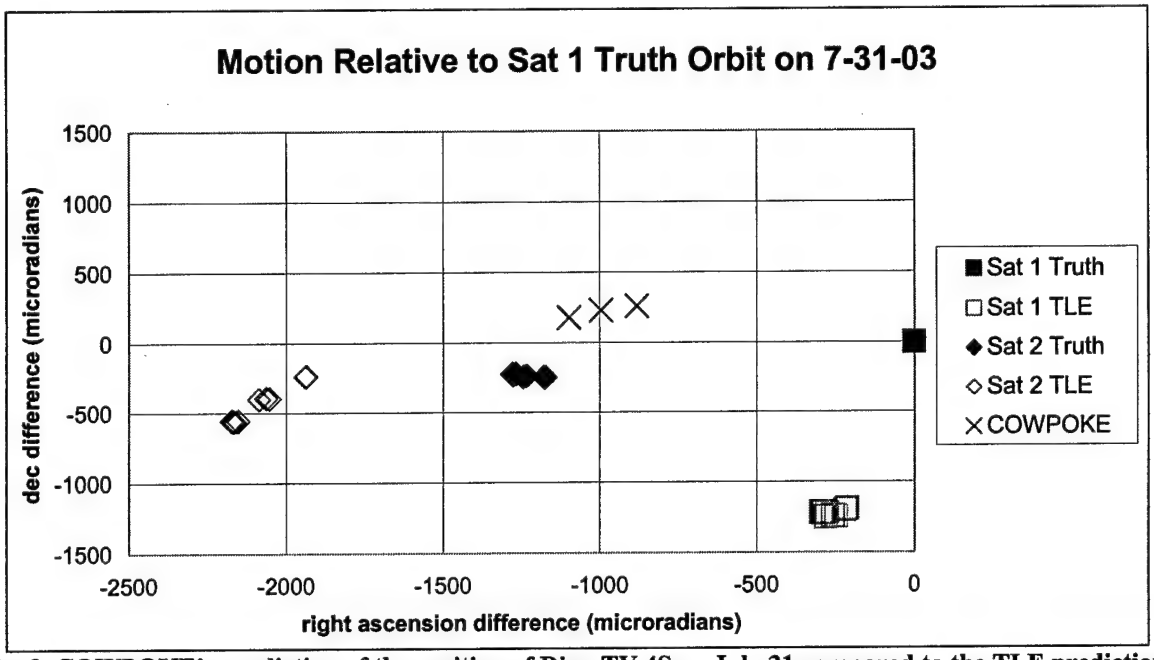

Fig. 8. COWPOKE's prediction of the position of DirecTV 4S on July 31 compared to the TLE predictions

Whatever the cause of the sudden shift, it was decided to start a new fit span. Only the observations from the night of the 31st were used to solve for the new element differences, and these were propagated forward with COWPOKE to the 1st of August. The COWPOKE and TLE predictions for that night are compared to the observations in Fig. 9. COWPOKE had an average error of 210 microradians, and the TLE for Sat 2 averaged 958 microradians. One of the advantages of COWPOKE is that the effects of maneuvers can be mitigated by using a one day fit span while TLEs typically use a longer fit span and will suffer the effects of maneuvers continuously.

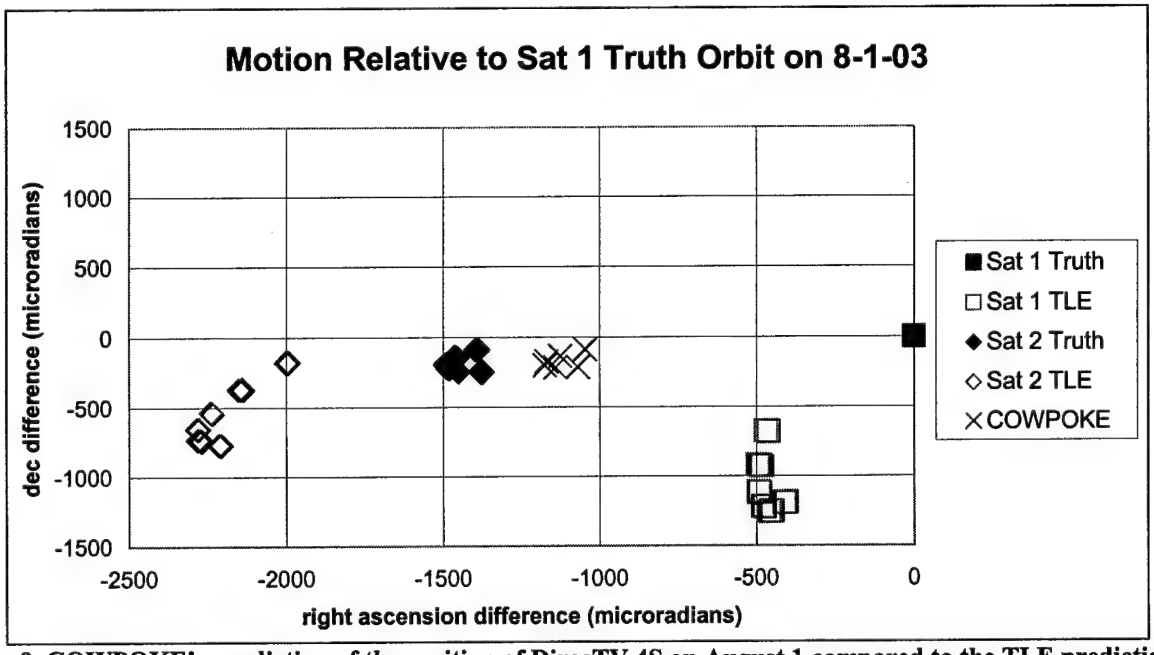

Fig. 9. COWPOKE's prediction of the position of DirecTV 4S on August 1 compared to the TLE predictions

While the COWPOKE results are somewhat encouraging when compared to the TLE's, the overall performance is not as good as expected. Perturbation analysis indicate that the equations should be accurate with only a few percent error. The simulation results showed similar error levels. If the relative orbit estimation algorithms were functioning properly, one would expect to see results with errors at the few percent level. For the one day fit cases shown in Fig. 5 and 9, larger errors might be expected due to limited observability over a short data arc. For the five day prediction case shown in Fig. 6, one might also expect to see larger errors due to the prediction interval. Then there is the case, shown in Fig. 8, where the reference satellite appears to maneuver; this would also cause prediction error. However, one case remains, shown in Figure 7, where several days of data are used in the estimation process and the prediction interval is only one orbit; the COWPOKE prediction error is as large as all of the other cases and is around 10% of the separation distance. This is larger than expected and indicates that there may be an unknown error source in the algorithm or software tools. Regardless, efforts must be made to better understand the limitations of this approach.

7. CONCLUSIONS AND FUTURE WORK

This work has shown that the COWPOKE equations can be used to provide meaningful relative motion of geosynchronous satellite clusters. Perturbation analysis indicated that 2-body dynamics are adequate for medium accuracy applications. Improvements were made to the equations, however, to account for large right ascension of the ascending node, argument of perigee, and true anomaly element differences.

Estimating the Keplerian element differences and using the COWPOKE equations to predict the relative motion can supply valuable information in spacecraft identification. Using six nights of Raven images, it is shown that COWPOKE estimated the position of DirecTV 4S relative to AMC-4 much better than TLE predictions, even with unmodeled maneuvers. This indicates that COWPOKE holds the potential to be a valuable space surveillance tool.

Sizable error still remains in the relative orbit prediction results. These errors are larger than anticipated so care must be taken to detemine the major source of this error and remove it. If this can be accomplished, the relative orbit estimation approach will be far more valuable. Beyond those improvements, the effects of differential SRP should be formulated for circular, equatorial orbits to better predict the motion of GEO clusters.

8. ACKNOWLEDGMENTS

Keric Hill was supported by the AFRL Space Scholars Program. Our sincere appreciation goes to Dr. Clifford Rhoades of AFOSR for funding Space Scholars at AMOS, and to Maj. Bill Hilbun, Ph.D., of AFOSR for funding the initial COWPOKE research. Thanks to Chuck Matson, Paul Kervin, Lt.C. Jeff McCann, Valerie Skarupa, TSgt. Khalid Golden, and Irma Aragon for supporting COWPOKE research at AMOS. Additional thanks to the Space Vehicles Directorate for administering and allowing AMOS's participation in the Space Scholars program.

---

9. REFERENCES

[i]. Pattinson, L., V. Chechik, "Eutelsat Satellite Collocation," AIAA/AAS Astrodynamics Specialist Conference, Quebec City, Canada, August 2001, AAS 01-317.

[ii]. Sabol, C., Burns, R., Wallace, S., "Analysis of the Telstar-401/GOES-10 Close Approach Using the Raven Telescope", AAS/AIAA Space Flight Mechanics Meeting, Monetery, CA, February 9-11, 1998, AAS 98-118.

[iii]. Abbot, R., R. Clouser, E. Evans, J. Sharma, "Close Geostationary Satellite Encounter Analysis: 1997-2001," AAS/AIAA Space Flight Mechanics Meeting, San Antonio, TX, 27-30 January 2002, AAS 02-115.

[iv]. Gist, R., D. Oltrogge, "Risk Management of Unintentionally Collocated Geosynchronous Spacecraft," AIAA/AAS Astrodynamics Specialist Conference, Quebec City, Canada, August 2001, AAS-01-321

[v]. Payne, T.E., Gregory, S.A., et al., "Space Object Identification of Geosynchronous Satellites," *Proceedings of the 1999 AMOS Technical Conference*, Maui, Hawaii, August-September 1999, pp. 195-203.

[vi]. Sabol, C., C. McLaughlin, K. Luu, "Meet the Cluster Orbits With Perturbations Of Keplerian Elements (COWPOKE) Equations," AAS/AIAA Spaceflight Mechanics Conference, Ponce, Puerto Rico, February 9-13, 2003, AAS-03-138.

[vii]. Sabol, C., Luu, K., Kervin, P., Nishimoto, D., Hamada, K., Sydney, P., "Recent Developments of the Raven Small Telescope Program," AAS/AIAA Space Flight Mechanics Meeting, San Antonio, Texas, January 2002, AAS 02-131.

[viii]. Law, B., et al, "The Phoenix System: Development of a Wide-Field Optical Sensor," *Proceedings of the 2002 AMOS Technical Conference*, Wailea, HI, 16-20 September 2002.

[ix]. Hill, K., et al, "Relative Orbit Trajectories of Geosynchronous Satellites using the COWPOKE Equations," *Proceedings of the 2003 AMOS Technical Conference*, Wailea, HI, 8-12 September 2003.

[x]. Sabol, C., S. Carter, and M. Bir, "Analysis of Preselected Orbit Generator Options for the Draper Semianalytic Satellite Theory," AIAA/AAS Astrodynamics Specialist Conference, Denver, Colorado, August 2000, AIAA-2000-4231.

[xi]. Vadali, R., "An Analytical Solution for Relative Motion of Satellites," DCSSS Conference, Cranfield University, Cranfield, UK, July 2002.

[xii]. Born, G., B. Tapley, B. Schutz, "Fundamentals of Orbit Determination, Class Notes for ASEN 5070." University of Colorado, Fall 2002.

[xiii]. Roy, A. E., *Orbital Motion*, J W Arrowsmith Ltd, Bristol, Great Britain, 1988.

Satellite Formation Flight Using the Perturbed COWPOKE Equations

Kathryn A. Catlin[xiii]
University of North Dakota, Grand Forks, North Dakota, 58202

The motion of satellites flying in formation around the Earth is ordinarily modeled by Hill's Equations of relative motion. Recently, Sabol et. al. developed a set of more intuitive equations, known as the Cluster Orbits With Perturbations Of Keplerian Elements (COWPOKE) Equations. To accurately model orbital motion, these equations must be modified to incorporate various perturbation effects, among them J_2 and drag. These effects have been added to the model, and simulations were run to compare this approach with "truth" orbits generated by Analytical Graphics, Inc.'s Satellite Tool Kit.

Nomenclature

δ	=	denotes differential
r	=	radial position, km
xt	=	cross-track position, km
at	=	along-track position, km
a	=	semimajor axis, km
e	=	eccentricity
M	=	mean anomaly, rad
v	=	true anomaly, rad
β	=	cross-track angular separation
α	=	along-track angular separation
Ω	=	right ascension of the ascending node, rad
ω	=	argument of perigee, rad
i	=	inclination, rad
n	=	mean motion, 1/sec
p	=	semilatus rectum, km
J_2	=	Earth oblateness parameter, .0010826269
$R_\oplus$	=	Earth radius, 6378.1363 km
$\dot{}$	=	denotes time derivative
μ	=	Earth gravitational parameter, 398600.4415 km^3/sec^2
t	=	time, seconds
$_o$	=	denotes initial condition
$_1$	=	denotes reference satellite
$_2$	=	denotes second satellite
ω_{xy}	=	placeholder for mean motion derivative
F_D	=	drag force, N
V	=	velocity magnitude, m/sec
BC	=	ballistic coefficient, kg/m^2
ρ	=	density, kg/m^3
m	=	mass, kg
C_D	=	drag coefficient

A		=	cross-sectional area, km^2
H		=	scale height, km
h_{ellip}	=	height above the ellipsoid, km	
h_o		=	reference height, km
ρ_o		=	reference density, kg/m^3

Introduction

SINCE 1878, the dominant equations of motion to describe relative satellite position and velocity have been Hill's Equations. Later modified by Clohessy and Wiltshire, these equations form the simplest, most basic model of satellite formation flight in use today. Of course, for most applications, a robust orbit propagator such as the Goddard Trajectory Determination System (GTDS) provides highly accurate, near-truth results. However, on some occasions, propagators are not available, or an analytical representation is simply preferred. It is in these instances that Hill's Equations are ordinarily used to model formation flight.

Hill's Equations, in their simplest form, are derived directly from the two-body equations of relative motion and do not include any orbital perturbations. Although it is possible to incorporate perturbations, the equations were intended to model the close approach of two satellites over a short period of time, not for indefinite periods as is the case for formation flight; the equations tend to break down over time. Hill's Equations assume that the orbit is circular and that the satellites are close together: although this works well for approach and rendezvous scenarios, the assumptions are not necessarily valid for most formation-flight applications. Also, while Hill's Equations follow naturally from the algebraic equations of motion of the satellites, the approach can be non-intuitive at best.

Recently, Sabol et. al. described a novel *geometric* approach to formation flight modeling: the Cluster Orbits With Perturbations Of Keplerian Elements, or COWPOKE, Equations.[1] Rather than using a Cartesian, satellite-centered reference frame, the COWPOKE Equations are based on a spherical Earth-centered frame and use known Keplerian orbital element differences to directly determine the cross-track, along-track, and radial separations between two satellites. Not only is this direct, geometric, Keplerian approach more intuitive than the algebraic Hill model, but because existing perturbation models are ordinarily given in terms of Keplerian element differences, integrating those models into the equations of motion is made considerably simpler.

Prior to this investigation, however, incorporation of any perturbations into the COWPOKE Equations had not been attempted; although Hill et al. have improved and extended the equations for use on geosynchronous orbit.[2] Here, I describe the steps taken to include both the J_2 (Earth oblateness) and atmospheric drag perturbations into the COWPOKE Equations, and compare the resulting propagations with those generated by Satellite Tool Kit's SGP4 propagator. I have also included in the Appendix a similar derivation for Hill's Equations with perturbations, although these results have not been correlated with the COWPOKE or STK propagations.

Approach

The improved COWPOKE Equations are as follows:

$$\delta r = \frac{(a+\delta a)(1-(e+\delta e)^2)}{1+(e+\delta e)\cos(M+2e\sin(M)+\delta\nu)} - \frac{a(1-e^2)}{1+e\cos(\nu)}$$

$$\beta = \frac{\delta xt}{r} = -2\sin\left(\frac{\delta\Omega}{2}\right)\sin(i)\cos\left(\omega+\frac{\delta\omega}{2}+M+2e\sin(M)+\frac{\delta\nu}{2}\right)$$

$$+\delta i\sin(\omega+\delta\omega+M+2e\sin(M)+\delta\nu) \qquad (1)$$

$$\alpha = \frac{\delta at}{r} = (\delta\omega + \delta\nu)\cos(\delta i) + \delta\Omega\cos(i)$$

where δr is the radial displacement, α and β are the along-track and cross-track angular separations, respectively, a is the semimajor axis of the reference satellite's orbit, e is its eccentricity, i its inclination, ω its argument of perigee, Ω its right ascension of the ascending node, M its mean anomaly, v its true anomaly, and r the radius. δat and δxt denote along-track and cross-track linear separations. For details on the derivation of these equations, see Refs. 1 and 2.

Addition of the J_2 (first-order Earth oblateness) perturbation effects secular changes in the right ascension of the ascending node, argument of perigee, and mean anomaly:

$$\begin{aligned}
\dot{\Omega} &= -\frac{3nR_\oplus^2 J_2}{2p^2}\cos i \\
\dot{\omega} &= \frac{3nR_\oplus^2 J_2}{4p^2}(4 - 5\sin^2 i) \\
\dot{M} &= \frac{3nR_\oplus^2 J_2\sqrt{1-e^2}}{4p^2}(2 - 3\sin^2 i)
\end{aligned} \tag{2}$$

where $n = \sqrt{\frac{\mu}{a^3}}$ is the mean motion, μ the Earth's gravitational parameter, p the semilatus rectum, J_2 the first-order Earth zonal harmonic coefficient, and $R_\oplus$ the Earth's radius.

An inspection of Equations 1, 2, and 3 will reveal that inserting these secular effects into the COWPOKE Equations requires deriving new expressions for the $\delta\Omega$, $\delta\omega$, and $\delta\nu$ terms. The $\delta\Omega$ term is found by the following method:

$$\begin{aligned}
\delta\Omega &= \Omega_2 - \Omega_1 \\
&= (\Omega_{2_o} + \dot{\Omega}_2 t) - (\Omega_{1_o} + \dot{\Omega}_1 t) \\
&= \delta\Omega_o + (\dot{\Omega}_2 - \dot{\Omega}_1)t \\
&\textit{where} \\
\dot{\Omega}_1 &= -\frac{3}{2}\sqrt{\frac{\mu}{a^3}}\frac{R_\oplus^2 J_2}{[a(1-e^2)]^2}\cos i \\
\dot{\Omega}_2 &= -\frac{3}{2}\sqrt{\frac{\mu}{(a+\delta a)^3}}\frac{R_\oplus^2 J_2}{\{(a+\delta a)[1-(e+\delta e)^2]\}^2}\cos(i+di)
\end{aligned} \tag{3}$$

where orbital elements of satellite 2 are expressed as the elements of the reference satellite plus a differential, and the subscript o denotes an initial given quantity. Similarly,

$$\delta\omega = \delta\omega_o + (\dot{\omega}_2 - \dot{\omega}_1)t$$

where

$$\dot{\omega}_1 = \frac{3}{4}\sqrt{\frac{\mu}{a^3}}\frac{R_\oplus^2 J_2}{[a(1-e^2)]^2}(4-5\sin^2 i) \tag{4}$$

$$\dot{\omega}_2 = \frac{3}{4}\sqrt{\frac{\mu}{(a+\delta a)^3}}\frac{R_\oplus^2 J_2}{\{(a+\delta a)[1-(e+\delta e)^2]\}^2}[4-5\sin^2(i+di)]$$

The true anomaly is a bit more difficult. True anomaly difference is approximated by a first order expansion in terms of eccentricity and mean anomaly:[2]

$$\delta\nu = \delta M + 2(e+\delta e)\sin(M+\delta M) - 2e\sin(M) \tag{5}$$

Therefore, to determine the change in true anomaly, the change in mean anomaly must first be derived. Since for no perturbations, $\dot{M} = n$, for the J_2 case, $\dot{M} = n + \dot{M}_{J_2}$, with $\dot{M}_{J_2}$ from Equation 2. We know that $n = \sqrt{\frac{\mu}{a^3}}$, so letting $\omega_{xy} = n + \dot{M}_{J_2}$, δM can be found as above:

$$\delta M = \delta M_o + (\omega_{xy_2} - \omega_{xy_1})t$$

where

$$\omega_{xy_1} = \sqrt{\frac{\mu}{a^3}}\left[1+\frac{3}{4}\frac{R_\oplus^2 J_2\sqrt{1+e^2}}{[a(1-e^2)]^2}(2-3\sin^2 i)\right] \tag{6}$$

$$\omega_{xy_2} = \sqrt{\frac{\mu}{(a+\delta a)^3}}\left\{1+\frac{3}{4}\frac{R_\oplus^2 J_2\sqrt{1+(e+\delta e)^2}}{\{(a+\delta a)[1-(e+\delta e)^2]\}^2}\left[2-3\sin^2(i+\delta i)\right]\right\}$$

All of these new element differences are inserted back into the original COWPOKE Equations (Eqn. 1), and if the only perturbation desired is J_2, the derivation stops here.

Incorporation of the atmospheric drag perturbation follows a similar course. The force of drag is

$$F_D = \frac{1}{2}\frac{\rho V^2}{BC} \tag{7}$$

with ρ the atmospheric density, V the along-track velocity, and BC, the ballistic coefficient of the satellite, equal to

$$BC = \frac{m}{C_D A} \tag{8}$$

where m is the satellite's mass, C_D is its drag coefficient, and A is its area normal to the velocity. Atmospheric density will, of course, vary throughout the satellite's orbit. There are a number of approximations in use to calculate density; I have selected a simple exponential model for purposes of this simulation, where

$$\rho = \rho_o^{-\frac{h_{ellip} - h_o}{H}} \tag{9}$$

with ρ_o and h_o reference density and reference altitude, h_{ellip} the actual attitude above the ellipsoid, and H the scale height. These quantities can be found in a table such as Table 8-4 in Reference 3.

Given Equations 7, 8, and 9, the variation of parameters method is used to determine the element differences due to drag:[4]

$$\begin{aligned}
da &= -\frac{\rho}{BC} a^2 \frac{(1+e^2+2e\cos\nu)^{\frac{3}{2}}}{(1+e\cos\nu)^2} d\nu \\
de &= -\frac{\rho}{BC} a(1-e^2) \frac{(1+e^2+2e\cos\nu)^{\frac{3}{2}}}{(1+e\cos\nu)^2} (\cos\nu + e) d\nu \\
di &= 0 \\
d\Omega &= 0 \\
d\omega &= -\frac{\rho}{BC} \frac{a(1-e^2)}{e} \frac{(1+e^2+2e\cos\nu)^{\frac{1}{2}}}{(1+e\cos\nu)^2} \sin\nu d\nu
\end{aligned} \tag{10}$$

Again, as above, the final Keplerian element differences become

$$\begin{aligned}
da &= da_o + (da_2 - da_1)t \\
de &= de_o + (de_2 - de_1)t \\
d\omega &= d\omega_{J_2} + (d\omega_2 - d\omega_1)t
\end{aligned} \tag{11}$$

where, again, the subscript o denotes an original given element difference, and $d\omega_{J2}$ is the argument of perigee difference due to Earth oblateness as found above. These final element differences are substituted back into Equations 1, and the derivation of the COWPOKE Equations with J_2 and atmospheric drag perturbations is complete. An examination of the Appendix should convince the reader that this method is considerably simpler than the incorporation of perturbations into Hill's Equations.

Methodology and Results

To validate and test the above derivations, simulations were run using a set of mean orbital elements with all element differences equal to .01. The elements and differences are given in Table 1.

The modified COWPOKE Equations are modeled in Matlab as above. The simulations run for 60 hours with data points taken at 1-minute intervals. To validate and verify the results, simulations are also run using STK's SGP4 propagator. In STK, the relative position of the two satellites is automatically calculated as a vector; the data is exported to Matlab and compared with the COWPOKE-derived orbit. For the drag perturbation, the mass of both satellites is taken to be 1000 kg and the cross-sectional area .000001 km^2. The drag coefficient of satellite 1 is 2, and the drag coefficient of the second satellite is slightly varied, at 2.001. This results in an approximate 250000 kg/km^2 difference in ballistic coefficient. These parameters are shown in Table 2.

Figures 1 through 3 show the radial, along-track, and cross-track differences, respectively, for both propagation methods; the second plot in each figure shows the error between COWPOKE and STK.

Table 1: Keplerian Elements and Element Differences

	Reference Elements	Element Differences
a (km)	T7000	.01
e	.01	.01
i (rad)	.785	.01
ω (rad)	0	.01
Ω (rad)	4.712	.01
M_o (rad)	1.751	.01

Table 2: Other Parameters Used for Propagation

Parameter	Value
Propagator	STK SGP4
Step Size (seconds)	60
Sat 1 mass (kg)	1000
Sat 2 mass (kg)	1000
Sat 1 area (km^2)	.000001
Sat 2 area (km^2)	.000001
Sat 1 drag coefficient	2
Sat 2 drag coefficient	2.001

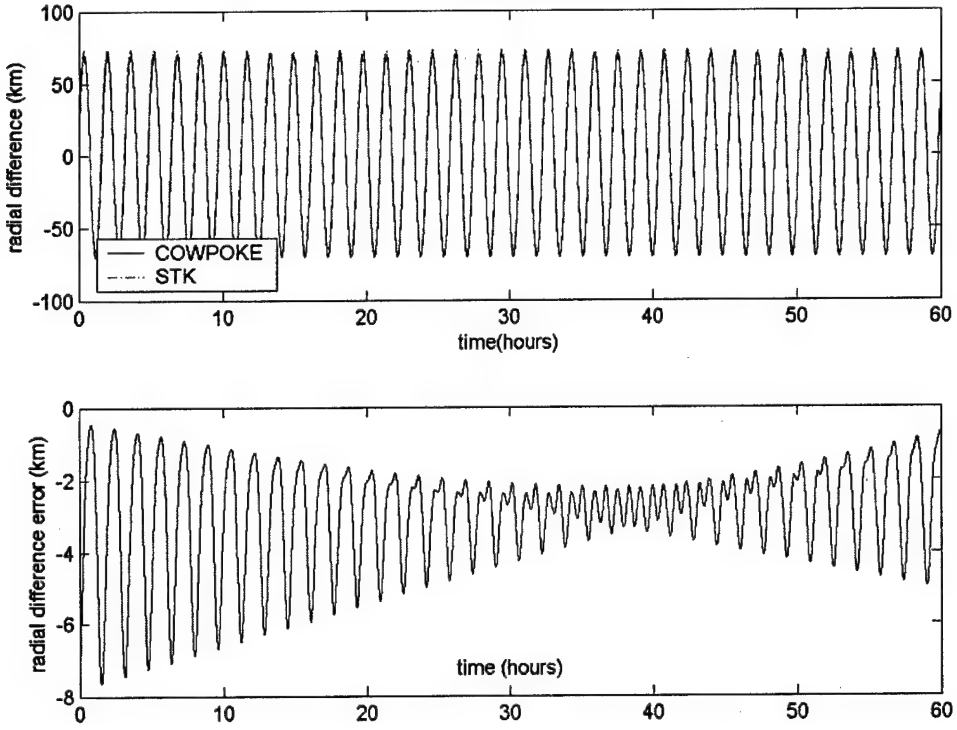

Figure 1: Radial Differences

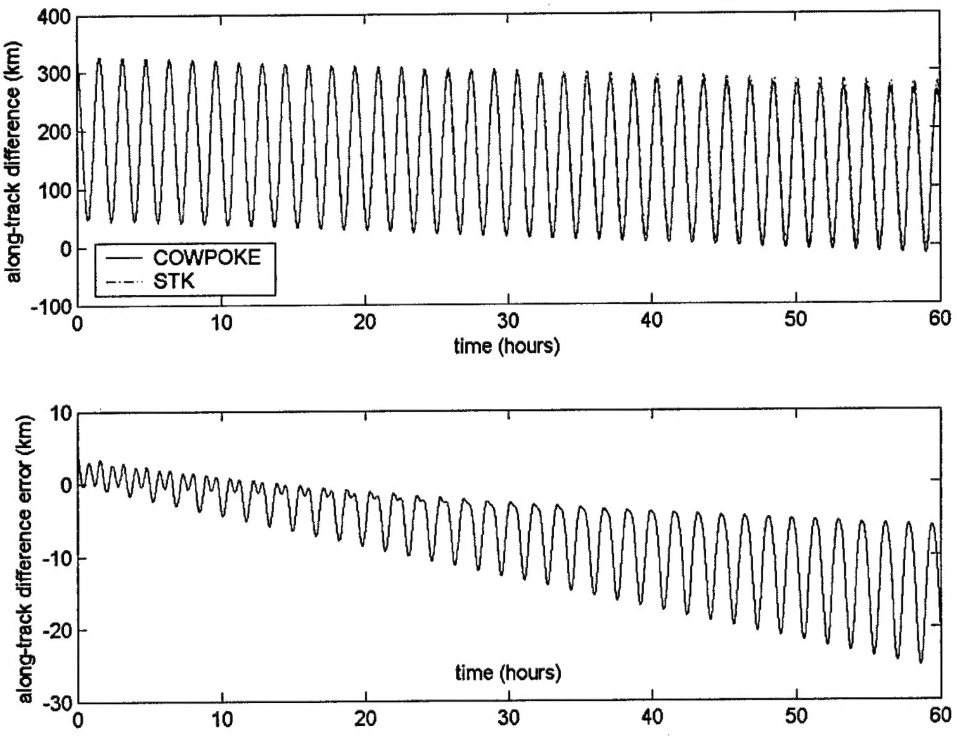

Figure 2: Along-Track Differences

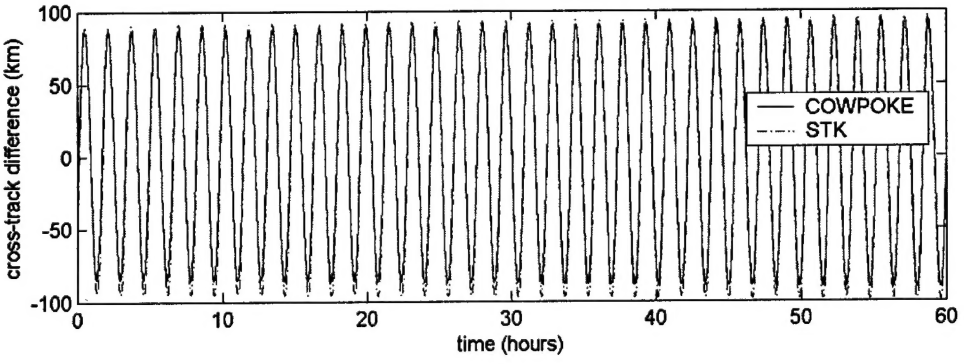

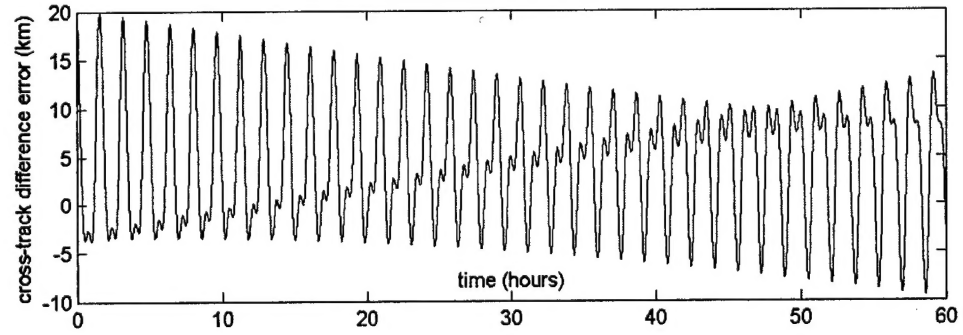

Figure 3: Cross-Track Differences

Conclusion

The COWPOKE Equations have been modified to include the effects of both zonal harmonic and atmospheric drag perturbations. This was expected to increase the accuracy of the equations with respect to a "truth" orbit as propagated by a commercial orbit integration program, rendering them more useful as a simple model of relative motion between satellites in formation flight scenarios. When compared to the orbit produced by STK's SGP4 propagator, the modified COWPOKE equations instead showed somewhat decreased accuracy. A number of reasons can be put forth for this, notably the different propagation methods used in this and previous papers. Before drawing a final conclusion about the modified COWPOKE Equations as here derived, a similar simulation should be run utilizing the GTDS software - the same propagator that was used in the original COWPOKE papers.[2] It would similarly be constructive to compare both the COWPOKE and STK results with the orbit defined by Hill's Equations with perturbations, which are derived in the Appendix. Furthermore, simulations should be run using observational data from real satellites to compare the COWPOKE results with reality. If, indeed, such research as indicated above should prove these modified COWPOKE Equations accurate and reliable, additional perturbations such as solar radiation pressure and third-body gravitational effects can be incorporated into the equations, further constraining the forces acting on the satellite and drawing the simulation ever closer to the actual, "truth" position of the orbit.

Appendix: Hill's Equations Solved with J_2 and Drag Perturbations

Hill's Equations solve the relative two-body equation of motion:

$$\ddot{\vec{r}}_{rel} = -\frac{\mu \vec{r}_1}{r_1^3} + \frac{\mu \vec{r}_2}{r_2^3} + \vec{F}_{other} \tag{12}$$

for two satellites traveling close to each other on a near-circular orbit. The equations are as follows:

$$\begin{aligned} \ddot{x} - 2\omega\dot{y} - 3\omega^2 x &= f_x \\ \ddot{y} + 2\omega\dot{x} &= f_y \\ \ddot{z} + \omega^2 z &= f_z \end{aligned} \tag{13}$$

where the *f*s are components of $\vec{F}_{other}$. The equations are solved many places, including Ref. 3; the position and velocity solutions are:

$$
\begin{aligned}
x(t) &= \frac{\dot{x}}{\omega}\sin(\omega t) - \left(3x_o + \frac{2\dot{y}_o}{\omega}\right)\cos(\omega t) + \left(4x_o + \frac{2\dot{y}_o}{\omega}\right) \\
y(t) &= \left(6\dot{x}_o + \frac{4\dot{y}_o}{\omega}\right)\sin(\omega t) + \frac{2\dot{x}_o}{\omega}\cos(\omega t) - (6\omega x_o + 3\dot{y})t + \left(y_o - \frac{2\dot{x}_o}{\omega}\right) \\
z(t) &= z_o\cos(\omega t) + \frac{\dot{z}_o}{\omega}\sin(\omega t) \\
\dot{x}(t) &= \dot{x}_o\cos(\omega t) + (3\omega x_o + 2\dot{y}_o)\sin(\omega t) \\
\dot{y}(t) &= (6\omega x_o + 4\dot{y}_o)\cos(\omega t) - 2\dot{x}_o\sin(\omega t) - (6\omega x_o + 3\dot{y}_o) \\
\dot{z}(t) &= -z_o\omega\sin(\omega t) + \dot{z}_o\cos(\omega t)
\end{aligned}
\tag{14}
$$

The secular effects of first-order zonal harmonics (J_2) on ω, Ω, and M are given in Equations 2. McLaughlin et. al.[5] have shown the method for introducing these secular variations into Hill's Equations, along with differential effects due to inclination differences between the two satellites.

Adding the drag perturbation to Hill's Equations is more complicated. In this drag-and-J_2-only case, f_x and f_z in Equation 13 are both zero, and f_y is equal to F_D, since the drag force acts only in opposition to the along-track velocity vector. Starting with Equation 7, a relative drag force is calculated by differencing the forces for the two satellites. Each individual parameter for the second satellite is expressed as the value for satellite 1 plus a differential. For example, V_2 is expressed as

$$V_2 = V_1 + \delta V \tag{15}$$

Simplifying and removing second-order and higher differentials from the resulting expression, the relative drag force can finally be expressed as

$$f_D = \frac{1}{2BC_1(BC_1 + \delta BC)}(2V_1\rho_1 BC_1\delta V + V_1^2 BC_1\delta\rho - V_1^2\rho_1\delta BC) \tag{16}$$

Setting f_y in Equation 13 equal to fD, and recognizing that the z force is uncoupled to the x and y components, the system of two equations can be solved. The solution process is as follows: Differentiate the x equation once, then solve via Laplace transforms, and differentiate the result to arrive and the x-velocity solution. The y equation can be solved by simple integrate. The resulting drag solution is then merged with the J2 solution[5] to arrive at the following set of equations describing the motion of one satellite with respect to another:

$$
\begin{aligned}
x &= \frac{\dot{x}_o}{\omega_{xy}}\sin\omega_{xy}t - \left(3x_o + \frac{2\dot{y}_o}{\omega_{xy}}\right)\cos\omega_{xy}t + 4x_o + \frac{2\dot{y}_o}{\omega_{xy}} \\
&\quad + \frac{t - \dfrac{1}{\omega_{xy}}\cos\omega_{xy}t}{\omega_{xy}BC\left(BC + \delta BC\right)}\left(2V\rho BC\delta V + V^2 BC\delta\rho - V^2\rho\delta BC\right) \\
y &= \left(6x_o + \frac{4\dot{y}_o}{\omega_{xy}}\right)\sin\omega_{xy}t + \frac{2\dot{x}_o}{\omega_{xy}}\cos\omega_{xy}t - 6\omega_{xy}x_o t - 3\dot{y}_o t + y_o - \frac{2\dot{x}_o}{\omega_{xy}} + a\left(\delta\dot{\Omega}\cos i + \delta\dot{\omega} + \delta\dot{M}\right)t \\
&\quad - \frac{\dfrac{3}{4}\omega_{xy}t^2 + 2t - \dfrac{2}{\omega_{xy}}\sin\omega_{xy}t}{\omega_{xy}BC\left(BC + \delta BC\right)}\left(2V\rho BC\delta V + V^2 BC\delta\rho - V^2\rho\delta BC\right) \\
z &= z_o\cos\omega_z t + \frac{\dot{z}_o}{\omega_z}\sin\omega_z t - a\delta\dot{\Omega}t\sin i\cos\omega_z t \\
\dot{x} &= \dot{x}_o\cos\omega_{xy}t - \left(3\omega_{xy}x_o + 2\dot{y}_o\right)\sin\omega_{xy}t \\
&\quad + \frac{1 + \sin\omega_{xy}t}{\omega_{xy}BC\left(BC + \delta BC\right)}\left(2V\rho BC\delta V + V^2 BC\delta\rho - V^2\rho\delta BC\right) \\
\dot{y} &= \left(6\omega_{xy}x_o + 4\dot{y}_o\right)\cos\omega_{xy}t - 2\dot{x}_o\sin\omega_{xy}t - 6\omega_{xy}x_o - 3\dot{y}_o + a\left(\delta\dot{\Omega}\cos i + \delta\dot{\omega} + \delta\dot{M}\right) \\
&\quad - \frac{\dfrac{3}{2}\omega_{xy}t + 2 - 2\cos\omega_{xy}t}{\omega_{xy}BC\left(BC + \delta BC\right)}\left(2V\rho BC\delta V + V^2 BC\delta\rho - V^2\rho\delta BC\right) \\
\dot{z} &= -\omega_z z_o\sin\omega_z t + \dot{z}_o\cos\omega_z t - a\delta\dot{\Omega}\sin i\left(\cos\omega_z t - t\omega_z\sin\omega_z t\right)
\end{aligned}
\tag{17}
$$

Despite the rather perfunctory treatment given the derivation in this Appendix, it should be clear from a glance at the preceding equations that working with the simple elegance of the COWPOKE Equations is eminently preferable to this mess, in addition to providing an inherently more accurate representation of relative satellite dynamics in a formation flight situation.

Acknowledgments

I would like to thank my advisor at the University of North Dakota, Dr. Craig A. McLaughlin, and the rest of the Space Studies Department at UND for their support and encouragement.

References

[1]Sabol, C., McLaughlin, C. A., and Luu, K. K., "Meet the Cluster Orbits With Perturbations Of Keplerian Elements (COWPOKE) Equations."

[2]Hill, K., Sabol, C., Luu, K. K., Murai, M. M., and McLaughlin, C., "Relative Orbit Trajectories of Geosynchronous Satellites Using the COWPOKE Equations."

[3]Vallado, D. A., *Fundamentals of Astrodynamics and Applications*, 2nd ed., Microcosm Press, El Segundo, CA, 2001, Chaps. 6, 8.

[4]Roy, A. E., *Orbital Motion*, 3rd ed., Student text, Adam Hilger, Bristol, 1991, Chaps. 6, 10.

[5]McLaughlin, C. A., Sabol, C., Swank, A., Burns, R. D., and Luu, K. K., "Modeling Relative Position, Relative Velocity, and Range Rate for Formation Flying," AAS 01-457.